

Refining the predictions of supersymmetric CP -violating models: A top-down approach

M. Argyrou¹, A. B. Lahanas¹, and V. C. Spanos²

¹ *University of Athens, Physics Department, Nuclear and Particle Physics Section, GR-15771 Athens, Greece*

² *University of Patras, Department of Physics, GR-26500 Patras, Greece*

Abstract

We explore in detail the consequences of the CP -violating phases residing in the supersymmetric and soft SUSY breaking parameters in the approximation that family flavour mixings are ignored. We allow for non-universal boundary conditions and in such a consideration the model is described by twelve independent CP -violating phases and one angle which misaligns the vacuum expectation values (VEVs) of the Higgs scalars. We run two-loop renormalization group equations (RGEs), for all parameters involved, including phases, and we properly treat the minimization conditions using the one-loop effective potential with CP -violating phases included. We show that the two-loop running of phases may induce sizable effects for the electric dipole moments (EDMs) that are absent in the one-loop RGE analysis. Also important corrections to the EDMs are induced by the Higgs VEVs misalignment angle which are sizable in the large $\tan\beta$ region. Scanning the available parameter space we seek regions compatible with accelerator and cosmological data with emphasis on rapid neutralino annihilations through a Higgs resonance. It is shown that large CP -violating phases, as required in Baryogenesis scenarios, can be tuned to obtain agreement with WMAP3 cold dark matter constraints, EDMs and all available accelerator data, in extended regions of the parameter space which may be accessible to LHC.

1 Introduction

Supersymmetry (SUSY) seems to be an indispensable ingredient of Superstring theories and supersymmetric extensions of the Standard Model (SM) have attracted the interest of physicists for more than two decades or so. Supersymmetric models are the only known extensions of the SM that are renormalizable field theories, bearing therefore the virtue that radiative corrections can be put under control and definite predictions can be made. On the other hand it is well known that these models are characterized by many arbitrary parameters, even in their most simplified versions, and therefore additional theoretical assumptions have to be invoked to lessen their number and build less proliferated models. The minimal supersymmetric standard model (MSSM) has the minimal physical content and it needs 124 parameters, a large number indeed. These are reduced to much fewer in the supergravity scenarios (mSUGRA), in which universal boundary conditions hold, which can be further reduced if additional assumptions are made, as for instance absence of generation mixings in the supersymmetric sector at the tree level and/or absence of CP-violating phases in the supersymmetric parameters which in the minimal much studied versions of SUSY are switched off. For a review on the availability and the description of the various models see Ref. [1] and references therein. A thorough account of the parameters describing the supersymmetric models and the issue of the CP-violating phases can be found in [2].

Supersymmetric models with CP-violating phases, other than this occurring in the Cabibbo-Kobayashi-Maskawa matrix (CKM), have been extensively studied in the past [3–8]. In the mSUGRA models there are only two observable phases, in addition to the CKM phase, which are tightly constrained by the EDM data. In more general cases however, when universal boundary conditions are abandoned, the number of phases is increased opening new possibilities that greatly affect phenomenology. The CP-violating phases residing in the supersymmetric parameters produce not only new phenomena, absent in minimal models, but also affect CP-conserving quantities, like the mass spectrum for instance, or have large impact on various particle processes being therefore of relevance in collider searches [9]. The reconstruction of the soft supersymmetric Lagrangian from experimental data, including cases where CP-phases are present is addressed in many works [10].

The constraints imposed by the EDM data of neutron [11], $|d_n| < 6.5 \times 10^{-26} \text{ e} \cdot \text{cm}$, the EDM of electron [12] deduced from measurement of the corresponding EDM of thallium, $|d_e| < 1.6 \times 10^{-27} \text{ e} \cdot \text{cm}$, or diamagnetic atomic systems such as Mercury (Hg-199) [13], $|d_{Hg}| < 2.1 \times 10^{-28} \text{ e} \cdot \text{cm}$, are very tight restricting CP-violating phases to be unnaturally small. This problem is termed as the supersymmetric CP-problem. The phenomenological constraints imposed by measurements of the electric dipole moments has been the subject of numerous works [3–6, 14–33]¹. To forbid overproduction of EDMs one may assume that the masses of superpartners are heavy enough beyond the reach of LHC. In other approaches special mechanisms are invoked, such as the cancellation mechanism [14–16, 18, 20], in which contributions of the various Feynman

¹For a thorough review concerning the role of dimension five and six operators affecting the EDMs of atomic systems and their link to EDMs of neutron and electron see [32]. For a general review concerning low energy tests of the weak interactions including EDMs see [33].

graphs involved delicately cancel each other to render EDMs of neutron and electron small within their experimental limits. However even in this case the limits imposed by the EDM of Mercury atom are hard to satisfy [19,21]. One may cure the situation by lifting the sfermion masses [22] but then two-loop contributions are not suppressed [23, 24]. The EDMs have been studied beyond the one-loop order. The Barr-Zee type [34] two-loop supersymmetric contributions have been thoroughly studied [25–29] and yield sizable contributions which do not decouple in the limit of heavy sfermion masses. The same holds even for some three-loop contributions arising from the running of the renormalization group equations (RGEs) which induce sizable phases to the gaugino masses [30].

The effect of supersymmetric phases in Higgs sector has been extensively studied [35–41] and will not be repeated here; for a review and see [42]. We merely state that their couplings to other particles differ from the CP-conserving case and that the CP-odd Higgs mixes with the CP-even mass eigenstates. Therefore, except their involvement to EDMs, in principle, they also affect neutralino relic densities and thus they are important for cosmological considerations.

Large phases residing in supersymmetric parameters are welcome for Baryogenesis which can occur either through Leptogenesis [43] or through a strong first order electroweak phase transition (for reviews see: [44]). Squark and slepton driven Baryogenesis requires a light stop, with mass $120 \text{ GeV} < m_{\tilde{t}} < m_t$, and in conjunction with the fact that the phase transition becomes too weak for Higgs masses larger than $\sim 120 \text{ GeV}$ it leaves a narrow window for successful baryon asymmetry [45–48]. Higgsino and Gaugino driven baryogenesis [49, 50] is an alternative. This effect is resonantly enhanced when the Higgsino mixing parameter μ is of the same order with the gaugino masses $M_{1,2}$, [51]. The relevant CP-phases are $\arg(\mu M_{1,2})$ and values in the range $\sim 10^{-2}$ are adequate to produce the observed baryon asymmetry of the universe if $|\mu| \simeq |M_{1,2}|$.

During the last years the WMAP3 [52–54] and SDSS [55] precise determination of the cosmological parameters has stimulated new interest and, in conjunction with the constraints put by the accelerator data, it points to a better understanding and more thorough treatment of supersymmetric models that violate CP. The Cold Dark Matter (CDM) relic density implied by the latest WMAP3 data [54] lies in the range $\Omega_{CDM} h_0^2 = 0.1045^{+0.0072}_{-0.0095}$ imposing severe constraints on CP-conserving supersymmetric models (for a review see [56]). The importance of the CP-phases in conjunction with Dark Matter (DM) observations has been the subject of many works [57]–[58], [50]. In these works the effect of the phases on the neutralino relic abundance is discussed observing the constraints put by accelerators in various supersymmetric scenaria. For a recent review see [58, 59].

In this work we focus on mSUGRA-type CP-violating models with minimal flavour violation (MFV) and seek regions of the parameter space which are compatible with cosmological and EDM constraints and all available accelerator data. In particular we refine the analyses of previous works by taking into account:

- i. The two-loop renormalization group running of all phases included which may induce sizable effects at low energies having large impact on EDMs. We show that even small phases at the unification scale are responsible of inducing large corrections saturating in

some cases the experimental limits put on EDMs. Such an effect was studied in [30] for the particular case of the trilinear soft scalar coupling, whose phase affects the phases of the gaugino masses. However other phases with phenomenological interest, notably the gluino phase, may influence EDMs, as we shall show, inducing non-vanishing phases for the remaining soft parameters.

- ii. Full treatment of the one-loop minimization conditions in the presence of CP-violating sources. The one-loop effective potential depends on these phases and correct treatment, taking into account all one-loop contributions, shows that a misalignment of the Higgs vacuum expectation values (VEVs) is induced which is phenomenologically important. It is worth noting that the relative angle between the Higgs VEVs cannot be rotated away, even if the Higgs mixing parameter is taken real, by proper $U(1)$ Peccei-Quinn or R-symmetries. The appearance of this phase is due to one loop corrections of the effective potential. The importance of this misalignment angle for phenomenology has been pointed out in previous works [60,61]. Here we refine previous analyses and in conjunction with i) we show that it induces phenomena which although in principle small may have large impact especially on the EDMs and the relic density of the lightest supersymmetric particle (LSP), which is assumed to be the lightest neutralino.
- iii. The effect of strong interaction phases which in principle do not affect electron's EDM at one-loop, such as the gluino phase. We show that, due to two-loop RGE running, this phase may induce CP-odd invariant phases at low energies, with important consequences for EDMs which are absent in the one-loop analysis. Such a phase is phenomenologically interesting since it is observable in gluino production and it is known to affect neutralino relic densities indirectly through its influence on the bottom mass corrections [62–66]. In this work we also argue that the appearance of such a phase may affect the top-down approach of the renormalization group running since it may give rise to large corrections for the bottom Yukawa couplings having as a consequence the appearance of Landau poles [67] in the large $\tan\beta$ regime.
- iv. The updated experimental value of the top mass is $m_t = 171.4 \pm 2.1 \text{ GeV}^2$, which affects the location and shape of the cosmologically allowed funnels which open in regions where an LSP pair annihilates through a Higgs resonance [70]. It is known that these funnels are very sensitive to the input top (and bottom) quark mass [71].

In our treatment we follow a top-down approach, which is the appropriate handling if the low energy physics has its origin at Planckian energies. In this sense CP-violating phases are not given at the Electroweak scale but are extracted after a two-loop running of the real and imaginary parts of all parameters involved, which are inputs at the unification scale. Under these circumstances it is interesting to explore where, and under which circumstances, cosmologically allowed regions naturally show up, in which the EDM constraints are satisfied, for large phases which are relevant for Baryogenesis and other phenomenological issues. In our study we pay

² The central value $m_t = 171.4 \text{ GeV}$ [68] of the top mass has slid down by 0.5 GeV according to more recent *CDF* and *D0* analyses [69]. Throughout this work the value $m_t = 171.4 \text{ GeV}$ is used.

special attention to the LSP pair annihilation through a Higgs resonance which is one of the leading mechanisms to produce the right amount for neutralino CDM especially in the large $\tan\beta$ regime.

In doing so, we have developed a Fortran numerical algorithm, which treats CP-violating sources in the MFV scenario in the approximation of neglecting generation mixings from the CKM matrix, whose effects are known to be small³. In this scheme soft masses and trilinear soft couplings are assumed diagonal in family space. In our study we discuss in detail the issues associated with the mass predictions of such models, focusing on a two-loop RGEs running and the effect of the CP-phases on quantities that greatly affect the renormalization group flow and the extracted low energy parameters. As has been already remarked, in our analysis electroweak radiative symmetry breaking is enforced with all one-loop contributions to the effective potential duly taken into account when CP-violations are switched on.

This paper is organized as follows. In Section 2 we give a detailed account of the role of the phases in conjunction with the class of models studied in this work. In Section 3 we discuss all subtleties associated with the phases that are involved and discuss all pertinent formulas which have a large impact on the numerical analysis. In Section 4 we discuss the importance of the energy dependence of the phases involved and in Section 5 we discuss the constraints arising from EDMs and Cosmology and present our main results. We end up with the conclusions in Section 6 and give a summary of our results.

2 Description of the Model

In the softly broken supersymmetric theory the Lagrangian is split as

$$\mathcal{L} = \mathcal{L}_{\text{SUSY}} + \mathcal{L}_{\text{soft}} ,$$

where all information concerning supersymmetry breaking is encoded in the soft part $\mathcal{L}_{\text{soft}}$. Proper U(1) and R-transformations of the multiplets involved may be used to eliminate some of phases residing in the parameters describing this Lagrangian leaving aside a number which cannot be further rotated away. These phases consist an additional set of arbitrary parameters with important phenomenological consequences. There are several works describing the situation in extensions of the MSSM, in which the presence of such phases is taken into account and their phenomenological implications are discussed. In this work we study MFV versions of supersymmetric models assuming that soft masses and trilinear couplings residing in $\mathcal{L}_{\text{soft}}$ are family blind. For brevity this class of models we shall coin CPMSSM. In such models the effects of the 1st and 2nd generation Yukawa couplings in the running of the renormalization group equations (RGE) is small and can be safely neglected from the analysis.

To start with, it may help to recall the basic field transformations used in order to eliminate the redundant phases of the various parameters involved. MSSM based models have $U_Q(3) \times U_{U_C}(3) \times U_D(3)$ and $U_L(3) \times U_{E_C}(3)$ global symmetries acting on the quark and lepton multiplets

³ It is customary in literature to term as MFV those models that allow generation mixings only from the CKM matrix.

which can be used to eliminate redundant phases and real parameter from the quark and lepton Yukawa couplings. At the end six real quark masses, three CKM angles and one CP-violating CKM phase are left which are measurable. Thus, in the approximation that the effect of the generation mixing is neglected we deal with real Yukawa couplings which are diagonal in family space. However in the limit that the Higgs multiplet mixing parameter $\mu = 0$ and the soft terms are neglected additional symmetries exist. These are Peccei-Quinn (PQ) global $U(1)_{PQ}$ symmetries and R-symmetries $U_R(1)$ under which the bosonic and fermionic components of the multiplets involved are transformed by appropriate phase factors. Under $U(1)_{PQ}$ the Higgs multiplets $H_{1,2}$ have charge 1, all quark and lepton multiplets have charge $-1/2$ and the vector multiplets are neutral, that is carry zero charge. On the other hand the R-charge of these multiplets is 1 for the scalar Higgses, $1/2$ for the scalar partners of the quarks and leptons and zero for the vector bosons. The corresponding Higgsinos, quark and lepton fermions have charges by one unit less while gauginos carry R-charge $+1$. In the literature are used instead the symmetries $U(1)_{PQ}$ and $U(1)_{R-PQ}$. Under the latter the scalar Higgses carry zero charge. A useful way to keep track of the changes implemented by these transformations is to assume that the Higgs mixing parameter μ , the Yukawa couplings $h_{t,b,\tau}, \dots$, the gaugino masses M_a , the Higgs scalar mixing parameter m_3^2 , the trilinear couplings $A_{t,b,\tau}, \dots$ and the squark and slepton masses squared $m_{\tilde{q},\tilde{l}}^2$ are spurion fields transforming in the way shown in Table 1, so that the Lagrangian \mathcal{L} is kept invariant. Phrased in another way, if a $U(1)_{PQ}$ or $U(1)_{R-PQ}$ transformation is carried out on the fields involved, i.e. $f \rightarrow \exp(iQ_f\alpha)f$, the parameters in the transformed Lagrangian appear multiplied by $\exp(-iQ\alpha)$, with Q the charge shown in Table 1. It is apparent that $U(1)_{PQ}$ affects only μ, m_3^2 , under which both have the same charge, and $U(1)_{R-PQ}$ affects μ , the gaugino masses and trilinear couplings. None of these affects the Yukawa couplings and the soft scalar masses which means that if real in one basis they remain real after $U(1)_{PQ}$ or $U(1)_{R-PQ}$ transformations. In a particular basis one exploits the aforementioned transformations to rotate away redundant phases of the parameters involved. Which ones is a matter of convention. However certain combinations of phases are invariant under these PQ and R-transformations and all physical quantities depend on linear combinations of these invariants. In the CPMSM twelve independent invariant combinations can be defined,

$$\arg(\mu M_a m_3^{2*}) \quad , \quad \arg(\mu A_i m_3^{2*}) \quad .$$

Any other invariant combination is expressed in terms of these.

As already discussed the Yukawa couplings can be taken real, positive or negative⁴. Moreover if they are real at one scale they remain real at all scales. The reason is that their RGEs are of the generic form $dh/d\ln Q = S h$, with S real. The slepton and squark soft masses can be also taken real since their imaginary parts are completely decoupled from the theory. In general the

⁴ In our convention the VEVs of the Higgses are $\langle H_1 \rangle = v_1$, $\langle H_2 \rangle = \exp(i\theta)v_2$, with $v_{1,2}$ real, and the superpotential, see A.1, is such that the running masses for the bottom and tau are $m_b = -h_b v_1$ and $m_\tau = -h_\tau v_1$. We assume $h_b, h_\tau < 0$ so that these are positive. Since $\langle H_2 \rangle$ is complex the top mass term is $h_t v_2 e^{i\theta} t t_c + (h.c.)$. The phase θ can be absorbed by a chiral rotation resulting to a positive top mass $m_t = h_t v_2$ if $h_t > 0$. We shall adhere to this convention in the following. This chiral rotation modifies other couplings, like gluino-top-stop for instance, which will appear to be θ dependent.

Parameter	$U(1)_{PQ}$ - charge	$U(1)_{R-PQ}$ - charge
μ	-2	2
$h_{t,b,\tau\dots}$	0	0
M_a	0	-2
m_3^2	-2	0
$A_{t,b,\tau\dots}$	0	-2
$m_{\tilde{q},\tilde{l}}^2$	0	0

Table 1: Parameters and their PQ , $R - PQ$ charges

Lagrangian part involving the scalar soft masses has the following form,

$$\mathcal{L}_{soft} = -\frac{1}{2} m_{ij}^2 s_i^* s_j + (h.c) \quad (1)$$

where summation over the squark, slepton and Higgs fields, denoted by s_i , is understood. The RGEs of m_{ij}^2 at two-loop order can be found in [72, 73]. In the MFV scenario the matrix m_{ij} is diagonal and therefore only the real parts of the diagonal elements m_{ii} participate in Eq. (1) and affect physical quantities. Their imaginary parts are decoupled. Thus, only $Re(m_{ii}^2)$ matter whose signs can be either (+) or (-). In most of the cases the (-) case leads to potentials breaking colour and/or lepton number, or being unstable, and therefore these cases are not phenomenologically interesting.

In order to choose a particular basis to work with, one can exploit the PQ symmetry to make m_3^2 real. In this basis the invariants under the remaining $U(1)_{R-PQ}$ symmetry are $arg(\mu M_a)$ and $arg(\mu A_i)$. Furthermore, by use of $U(1)_{R-PQ}$ one of the phases of μ , M_a , A_i can be rotated away and no further rotations are allowed. Which one is rotated away is a matter of choice. For instance in mSUGRA, in the presence of CP-violation and with universal boundary conditions, one usually chooses to eliminate the phase of common gaugino mass, $M_{1/2}$, at the unification scale and two phases remain, this of μ and that of the common trilinear coupling A_0 . Since it is customary in mSUGRA to work in the basis in which μ , A_0 are complex it is advisable that we work in a basis where the phase of μ is not rotated away either, offering the opportunity of a direct comparison of CPMSSM with mSUGRA models. Also since in the EDM cancellation mechanism, to be described later, we implement rotations of the phases of M_1 and M_3 , in order to obtain values for the EDMs of electron and neutron much smaller than their experimental bounds, we had better not rotate away these two phases either.

One should take care of the fact that, in general, phases run with the energy scale. Thus, if a phase is set to zero at some energy scale, it may reappear at some other scale due to the RGE running. Exception to that are the Yukawa couplings and the μ parameter whose RGEs are multiplicative, by real functions, at any loop order. The RGEs of the soft gaugino mass parameters are multiplicative at one-loop, but not at the two-loop order, while those of the trilinear couplings are not multiplicative already at one-loop order. Therefore, more phases are expected to be generated through the RGE running even if at some scale they are vanishing. In mSUGRA like models, for instance, three phases are generated for the $M_{1,2,3}$ gaugino masses at low energy scales, due to the two-loop running, even if some of those are set to zero at the

unification scale. We shall discuss this issue in detail later on.

Except the phases associated with the parameters mentioned above, one further phase emerges, through loop effects. This is the misalignment angle of the Higgs VEVs which is present even if m_3^2 is chosen real. To maintain both Higgs VEVs real at one-loop an additional rotation of the Higgs fields should be performed, but then this relative phase moves someplaces else affecting other parameters. In our approach we take m_3^2 real at the minimization scale Q_{\min} , usually taken to be the average stop mass, by an appropriate PQ rotation. The reality of m_3^2 simplifies the solution of the minimization conditions as we shall discuss. In addition one can exploit the $U_Y(1)$ gauge symmetry of the Lagrangian to redefine fields in such a way that the VEV of H_1 is real. Thus, one has $\langle H_1 \rangle = v_1$ and $\langle H_2 \rangle = \exp(i\theta) v_2$, with $v_{1,2}$ both real. In general they can be taken both complex, $\langle H_i \rangle = \exp(i\chi_i) v_i$, $i = 1, 2$, but only the combination $\chi_1 + \chi_2 = \theta$ is observable. In the following we shall work in the basis in which $\langle H_1 \rangle$ is real. In this basis it is more appropriate to incorporate θ with the phase ϕ_μ of μ and use the combinations $\arg(\mu M_a \exp(i\theta)) = \phi_\mu + \xi_a + \theta$, and $\arg(\mu A_i \exp(i\theta)) = \phi_\mu + \phi_{A_i} + \theta$ to express physical observables. The reason of doing that is that chargino, neutralino and sfermion masses, as well as the EDMs of fermions, the quark chromoelectric moments, and the dimension-6 Weinberg operator, depend on the combination $\phi_\mu + \theta$ rather on ϕ_μ alone [16].

In our treatment we take m_3^2 and $\langle H_1 \rangle$ real at the minimization scale, as we discussed earlier, but we do not implement a further $U(1)_{R-PQ}$ transformation to rotate away one of the remaining phases at Q_{\min} . The reason is that even if any of these is rotated out at Q_{\min} , it will reappear at the unification scale M_{GUT} , with the exception of the phase of μ , due to the RGE running. Therefore we found it more convenient to deal with all thirteen phases, those of μ, M_a, A_i at M_{GUT} . The phase of m_3^2 at M_{GUT} and the misalignment angle of the VEVs, θ , are calculable and not free parameters. Although legitimate, in this procedure different choices for the input phases at M_{GUT} may correspond to the same physical situation. Therefore for given SUSY inputs we compare the values of $\arg(\mu M_a \exp(i\theta))$ and $\arg(\mu A_i \exp(i\theta))$ at Q_{\min} and θ after each run. If they coincide they correspond to the same physical situation and should not be double counted.

Supersymmetric CP-violation has important phenomenological implications and in conjunction with other cosmological and experimental constraints deserves further detailed study. For a review see [1] and references therein. The presence CP-violating phases affects the cosmological predictions for the neutralino relics which are the leading candidates for CDM. They have large impact on the bottom mass corrections, Δm_b , which in turn affects drastically the predicted neutralino relic density $\Omega_{\tilde{\chi}} h_0^2$. This effect is more enhanced for large values of $\tan \beta$, and for small trilinear scalar couplings the important phases are those of the parameter μ and the phase ξ_3 of the gaugino mass M_3 , [62–64]. For large values of the trilinear couplings, at low energy scales, their phases play a significant role also. The appearance of phases greatly affects the masses of the Higgs bosons as well, and thus they have a large impact on the DM predictions for neutralino annihilations near a Higgs resonance region, which is one of the regions favoured by the cosmological data. In [66] particular extensions of the mSUGRA, where the magnitudes of the soft breaking parameters are universal but their phases are different in general, were found

to be consistent with EDMs, WMAP3 data, $b \rightarrow s\gamma$ and $b - \tau$ Yukawa unification in regions of the parameter space in which the phases ϕ_μ, ξ_3 have large values. In these considerations the cancellation mechanism among the various contributions to EDMs was invoked [14–16, 18, 20], which proved to be a powerful tool to comply with EDM constraints, in the low $m_0, M_{1/2}$ regime, relaxing the stringent constraints imposed on the CP-violating phases although its validity and naturalness have been questioned in other works [19].

In this work we shall refine the analysis of the CP-violating models, focusing on mSUGRA-type models in which all phases are opened up, but magnitudes of the SUSY parameters are universal at the unification scale. These models are a subclass of the CPMSSM, and their phenomenology has been studied. However the subtleties associated with the two-loop running of all phases involved, in conjunction with the delicate treatment of the misalignment angle of the Higgs VEVs, which arises from the one-loop effective potential, have not been fully treated. The effects arising from such a consideration are important for EDMs and relic densities as we shall discuss.

3 CP-violation in the top-down approach

In the extended class of supersymmetric models discussed in the previous section, and in order to obtain the mass spectrum and phases at low scales one has to run seventy eight (78) RGEs for the real and imaginary parts of all quantities involved, including those of the six trilinear scalar couplings of the first two generations which are important for the study of the EDMs of the light fermions since they are affected by the gaugino masses and the trilinear couplings of the third generation species. Due to this dependence non-vanishing phases for these trilinear couplings can be developed, even if they are absent at the unification scale, affecting the EDMs of the light leptons and quarks with important phenomenological consequences.

The RGEs for the gauge couplings are certainly real and the Yukawa couplings can be taken real as explained in the previous section. The imaginary parts of the soft squark, slepton and Higgs masses run with the energy scale but as stated in the previous chapter have no effect on physics. Any choice for them leads to the same physical results and for convenience we take them zero at the unification scale. The RGEs, up to two-loop order, can be found in [72] and [73] and have been adapted to our own notation (see Appendix). These are run from a GUT scale M_{GUT} defined to be the point at which the gauge couplings $\alpha_{1,2}$ unify. We do not enforce unification of these with the strong coupling constant although it is left as an option in our numerical code. In this procedure we observe radiative electroweak symmetry breaking conditions which are altered in the presence of CP-violating sources. The Yukawa couplings of the first two generations have little effect and can be neglected from the remaining RGEs in the approximation that the third generation Yukawa's dominate.

In our analysis we follow a top-down approach with input values for the magnitudes and the phases of the soft masses and trilinear couplings at the GUT scale. The reasoning behind this relies on the fact that these are not known at low energies but they are rather determined from the fundamental underlying theory, which describes physics at GUT or Planckian energies.

As explained in the previous section we shall work in the basis in which by appropriate

$U(1)_{PQ}$ symmetry the Higgs mixing parameter m_3^2 is real at the minimization scale Q_{min} which we choose to be the average stop masses scale $Q_{\bar{t}} = (m_{\bar{t}_1} m_{\bar{t}_2})^{1/2}$. The neutral Higgses develop VEVs along the directions $\langle H_1 \rangle = v_1$, $\langle H_2 \rangle = v_2 e^{i\theta}$ and it is convenient to shift the neutral Higgs components as

$$H_1 = v_1 + \frac{R_1 + iI_1}{\sqrt{2}}, \quad H_2 = e^{i\theta} \left(v_2 + \frac{R_2 + iI_2}{\sqrt{2}} \right). \quad (2)$$

As in the CP-conserving case we write $v_1 \equiv \frac{v}{\sqrt{2}} \cos \beta$, $v_2 \equiv \frac{v}{\sqrt{2}} \sin \beta$ by defining the angle β . The misalignment angle θ is determined by minimizing the scalar potential and it is vanishing at the tree level. The minimization conditions are then given by

$$\begin{aligned} \frac{1}{2} (M_Z^2 + \Pi_{ZZ}) &= \frac{\bar{m}_1^2 - \bar{m}_2^2 \tan \beta^2 \cos^2 \theta}{(\tan \beta^2 - 1)(c_\beta^2 + s_\beta^2 \cos^2 \theta)} \\ \sin 2\beta &= - \left(\frac{c_\beta^2 + s_\beta^2 \cos^2 \theta}{\cos \theta} \right) \frac{2 m_3^2}{\bar{m}_1^2 + \bar{m}_2^2} \\ m_3^2 \sin \theta &= \frac{1}{\sqrt{2} v_2} \frac{\partial \Delta V}{\partial I_1}. \end{aligned} \quad (3)$$

In the equations above $c_\beta \equiv \cos \beta$, $s_\beta \equiv \sin \beta$, ΔV is the loop corrected scalar potential, and

$$\bar{m}_i^2 \equiv m_i^2 + \frac{\partial \Delta V}{\partial (Re H_i^0)^2}.$$

In the first of Eqs 3, M_Z is the physical (pole) Z-boson mass and $\Pi_{ZZ}(k)$ is the transverse Z-boson propagator correction at $k^2 = M_Z^2$. Its inclusion is important for a correct numerical treatment. Note that the expression on the l.h.s. in the first of Eq. 3 defines the squared of the running Z-boson mass, $\hat{M}_Z^2 = M_Z^2 + \Pi_{ZZ}$, which is used to derive the relations of $v_{1,2}$ with the other quantities. When the CP-violating phases are switched off the third of the equations above yields a vanishing misalignment angle θ , since its r.h.s. vanishes at the minimization point $I_i, R_i = 0$. In this case the first two of Eqs. 3 receive their well-known expressions valid in the CP-conserving case. In our treatment all one-loop corrections to the effective potential ΔV have been calculated allowing for CP-violating sources in the field dependent masses of all SUSY sectors involved, i.e. sfermions, charginos, neutralinos and Higgses.

In our numerical approach we have $\tan \beta$ as input and the value of m_3^2 at the minimization scale is determined by the second of Eqs. 3. The magnitude of μ parameter is output determined by the first of Eqs. 3. Recall that $m_i^2 = |\mu|^2 + m_{H_i}^2$, $i = 1, 2$, with m_{H_i} denoting the soft Higgs masses. In the presence of CP-violating sources the phase θ is non-vanishing, because of loop corrections to the effective potential, and it is determined from the third of Eqs. 3 (see [60,61]). Thus, it is expected to be small but its impact on the electric dipole moments of known species may be sizable. Since this is a one-loop quantity one can consistently solve Eq. 3 by putting $\theta = 0$ within ΔV .

The fields $R_{1,2}, I_{1,2}$ in Eq. 2 are not mass eigenstates. A linear combination of $I_{1,2}$, namely $I'_2 = -c_\beta I_1 + s_\beta I_2$ is the Goldstone mode and the orthogonal to it, $I'_1 = s_\beta I_1 + c_\beta I_2$, gets mixed

with $R_{1,2}$ through a 3×3 mass matrix. When CP violating effects are absent this matrix does not allow mixing of I'_1 with $R_{1,2}$. In this case I'_1 is the pseudoscalar, CP-odd, mass eigenstate. The other modes $R_{1,2}$ do get mixed and they must be rotated to yield the heavy and light CP-even mass eigenstates .

The corrections to the masses of the third generation, through which the corresponding Yukawa couplings are read, are very important and affect the numerical treatment. The presence of CP violating sources affects these corrections substantially. The supersymmetric corrections to the bottom mass are sizeable for large values of $\tan \beta$ and should be duly taken into account in the analysis. These give rise to large corrections to the bottom Yukawa coupling [74–76] given by

$$|\hat{h}_b| = \frac{\hat{m}_b^{SM}(M_Z)}{v_1} (1 + \Delta_{SUSY}^b)^{-1} . \quad (4)$$

Throughout with hat we denote quantities in the \overline{DR} scheme. In the equation above the SUSY corrections are denoted by Δ_{SUSY}^b and they are resummed according to the scheme presented in [75]. In this equation $\hat{m}_b^{SM}(M_Z)$ is the Standard Model \overline{DR} value of the bottom running mass at the scale M_Z . Its value is calculated by running the $SU_c(3) \times U_{em}(1)$ RGEs⁵ for masses and couplings in the \overline{MS} scheme, from the bottom mass $\hat{m}_b^{SM}(m_b) = 4.25 \pm 0.15$ GeV [78], as determined in lattice calculations, up to the scale M_Z . Its \overline{MS} value at M_Z is subsequently converted to its \overline{DR} value using well-known expressions. Therefore from Eq. (4) the value of \hat{h}_b can be extracted which is needed to run the RGEs from M_Z to the GUT scale. The corrections involved within Δ_{SUSY}^b are very important and are discussed below.

The leading supersymmetric QCD, sbottom-gluino, and Electroweak (EW), stop-charginos, contributions to Δ_{SUSY}^b are given by

$$\begin{aligned} \Delta_{SUSY}^b = & \frac{2\alpha_s}{3\pi} M_{\tilde{g}} (|\mu| \tan \beta \cos(\xi_3 + \phi_\mu + \theta) + |\mu| |A_b| \cos(\xi_3 - \phi_b)) G(\tilde{b}_1, \tilde{b}_2, M_{\tilde{g}}) \\ & - \frac{h_t^2}{16\pi^2} |\mu| (|\mu| + |A_t| \tan \beta \cos(\phi_\mu + \phi_t + \theta)) G(\tilde{t}_1, \tilde{t}_2, |\mu|) . \end{aligned} \quad (5)$$

$|A_{b,t}|, |\mu|$ are the magnitudes of $A_{b,t}, \mu$ and $\phi_{b,t}, \phi_\mu$ their phases. θ is the misalignment angle between the Higgs VEVs and tilded quantities denote sbottom, stop masses⁶. In this expression we have neglected electroweak (EW) mixings of the stops, and also sbottoms, and the mass of the chargino is put to μ . More refined expression which take into account the mixings can be found in ref [76]. An analogous treatment holds for the corrections to the tau mass as well. However their effect is small due to the absence of QCD corrections at the one-loop level. When the magnitudes of the trilinear couplings involved in Eq. 5 are small and the angle θ , which is anyway small, are neglected then this equation receives a much simpler form

$$\begin{aligned} \Delta_{SUSY}^b = & \frac{2\alpha_s}{3\pi} M_{\tilde{g}} |\mu| \tan \beta \cos(\xi_3 + \phi_\mu) G(\tilde{b}_1, \tilde{b}_2, M_{\tilde{g}}) \\ & - \frac{h_t^2}{16\pi^2} |\mu|^2 G(\tilde{t}_1, \tilde{t}_2, |\mu|) . \end{aligned} \quad (6)$$

⁵ In our treatment we use 3-loop QCD and two-loop QED RGEs for the strong and electric couplings and two-loop for the running masses of the bottom and tau. Four-loop, $\mathcal{O}(\alpha_s^4)$, QCD contributions to beta functions and quark anomalous dimensions are available [77] but affect little our analysis.

⁶The function $G(a, b, c)$ is identical to $I(a, b, c)$ defined in Eq. 7 in [75].

The functions G appearing in Eq. 6 are positive in a large portion of the parametric space and therefore if $\cos(\xi_3 + \phi_\mu)$ is negative the corrections to Δ_{SUSY}^b may turn out to be negative and sizable, in the large $\tan\beta$ regime. In this case the bottom Yukawa coupling of Eq. 4 gets large and a Landau pole may develop. Therefore in the top-down approach, depending on the inputs, the approach to the large $\tan\beta$ regime is not guaranteed. This observation is important for the mechanism of neutralino annihilation through a Higgs resonance, which opens for large values of $\tan\beta$. The importance of this will be discussed later.

The Yukawa coupling of the top quark is large and it is determined from the experimentally measured top pole mass in the following way. For the top quark the relation between its pole and running mass, including the dominant QCD and the supersymmetric gluino-stop corrections is given by

$$M_t^{pole} = m_t(M_t^{pole})(1 + \Delta_{SUSY}^t)/(1 - \Delta_{QCD}) . \quad (7)$$

The pole mass is scheme independent so that the r.h.s can be calculated in either \overline{MS} or \overline{DR} scheme. We prefer to employ the first scheme since the QCD corrections Δ_{QCD} have a simple form which at two-loops is given by

$$\Delta_{QCD} = \frac{4}{3\pi}\alpha_s + 1.11\alpha_s^2 . \quad (8)$$

In Eq. 8 the strong coupling constant is meant at M_t^{pole} and its running from any lower scale to the pole top mass is done using the five quark flavour RGEs. Note that in Eq. 7 the QCD corrections have been resummed. The \overline{MS} strong coupling α_s appearing in the above expressions is different from the corresponding \overline{DR} strong coupling usually denoted by α_3 . The relation between these two will be given in the sequel.

The gluino-stop corrections appearing in Eq. 7 are given by

$$\begin{aligned} \Delta_{SUSY}^t &= \frac{\alpha_s}{3\pi} [-B_1(0, M_{\tilde{g}}, m_{\tilde{t}_1}) - B_1(0, M_{\tilde{g}}, m_{\tilde{t}_2}) \\ &\quad - \frac{M_{\tilde{g}}}{m_t(M_t^{pole})} \sin(2\theta_t) \cos\xi (B_0(0, M_{\tilde{g}}, m_{\tilde{t}_1}) - B_0(0, M_{\tilde{g}}, m_{\tilde{t}_2}))] \end{aligned}$$

In this θ_t is the angle diagonalizing the stop mass matrix, $\xi \equiv \xi_3 + \phi + \theta$ and $m_{\tilde{t}_{1,2}}$ are the stop masses ⁷. This generalizes the results of ref. [79] in the case that the supersymmetric parameters are complex. The functions $B_{0,1}$ are defined as in [79]. A minus sign difference with the results of that reference, occurring in the case of the absence of CP violations, $\xi = 0$, is due to the slightly difference notation used here. Note that these corrections have the same form in both \overline{MS} and \overline{DR} schemes since in the gluino-stop loop scalar particles are exchanged and no traces of gamma matrices are involved. Their difference in the two schemes is therefore small, two-loop, due to the fact that the couplings and running masses appearing already differ at

⁷ The diagonalizing matrix K is defined by $K M^2 K^\dagger = \text{diag}(m_{\tilde{t}_1}^2, m_{\tilde{t}_2}^2)$ with the matrix elements of K given by $K_{11} = K_{22} = \cos\theta_t$, $K_{12} = -K_{21}^* = e^{i\phi} \sin\theta_t$. The definition of the matrix K we adopt is consistent with K tending to the unit matrix if the off-diagonal elements of the squark mass matrix are switched off. Thus, the subscripts in $m_{\tilde{t}_{1,2}}$ do not specify the ordering of their heaviness.

one-loop in the two schemes. More refined relations including the subdominant EW corrections are given in [76]. The EW supersymmetric corrections are however small and they correct the approximate result by less than 1% which becomes even less when the stop masses are of the order of 1 TeV. Therefore the \overline{MS} value for the top Yukawa coupling is given by

$$h_t^{\overline{MS}}(M_t^{pole}) = \frac{M_t^{pole}}{v_2} \frac{1 - \Delta_{QCD}}{1 + \Delta_{SUSY}^t} \Big|_{\overline{MS}} \quad (9)$$

and its \overline{DR} value needed to run the corresponding RGEs is provided by the usual conversion formula [80]

$$h_t^{\overline{MS}}(M_t^{pole}) = h_t^{\overline{DR}}(M_t^{pole}) \left(1 + \frac{\alpha_3}{8\pi} + \frac{\alpha_2}{16\pi} + \frac{3\alpha_1}{80\pi} \right) . \quad (10)$$

Besides the input Yukawa couplings, we need the values of the gauge couplings at the unification scale M_{GUT} defined to be at the point where the gauge couplings $\alpha_{1,2}$ meet. These are determined by their values at the scale M_Z in terms of the fine structure constant α_0 , the value of the Fermi coupling constant G_F and the physical Z-boson mass M_Z . These are related to $\alpha_{1,2}(M_Z)$ in the way prescribed in [79]. These are run up by two-loop RGEs and the unification scale M_{GUT} is determined at the point where these intercept. Naive gauge coupling unification would entail to putting the strong coupling α_3 equal to $\alpha_{1,2}$ at M_{GUT} . Instead of doing this we follow the alternative, followed in [79], according to which the \overline{MS} value of the strong coupling, denoted by α_s , coincides with the one experimentally measured. Its relation to α_3 at the scale M_Z is given by

$$\alpha_s(M_Z) = \alpha_3(M_Z)/(1 - \Delta\alpha_3)$$

where $\Delta\alpha_3$ includes supersymmetric threshold corrections and constants associated with passing from \overline{MS} to \overline{DR} scheme. This determines α_3 . The Yukawa and gauge couplings determined at lower scales in the way prescribed earlier are run up at M_{GUT} to determine their values at the unification scale. This is done iteratively until a certain convergence is achieved. In our code the Higgsino and Higgs mixing parameters μ, m_3^2 are outputs, and the convergence criteria in our numerical code are tailored to monitor these parameters in each iteration, which in most of the cases have the slowest convergence from the other parameters involved. In determining these we use the full one loop effective potential with the leading two-loop QCD correction taken into account. The minimization conditions are considered at an average stop scale as described earlier and the Higgs mixing parameter m_3^2 is taken real without loss of generality as we have discussed. At any other scale, including the unification, this is certainly complex and its phase is extracted from the running of the RGEs from the minimization scale.

Concerning the mass spectrum of SUSY particles the gluino physical mass is overwhelmed by large QCD corrections which affect the numerical analysis and should be discussed. These are due to both SM gluon exchanges and supersymmetric corrections due to exchanges of fermions and their corresponding squarks. The relation between the physical, $M_{\tilde{g}}$, and the soft gluino mass, M_3 , is found to be

$$M_{\tilde{g}} = \frac{|M_3(Q)|}{(1 - 3\alpha_3(Q) (5 + 6 \ln(Q/|M_3(Q)|) - S(Q))/(4\pi))} \quad (11)$$

where α_3 is the \overline{DR} value of the strong coupling and $S(Q)$ the squark contribution given by

$$S(Q) = \frac{1}{3} \sum_{i=1}^3 (2\tilde{q}_i + \tilde{u}_i + \tilde{d}_i) . \quad (12)$$

In $S(Q)$ \tilde{q}_i denotes the contribution of the squark doublets, accommodating the left-handed up and down squarks, and \tilde{u}_i, \tilde{d}_i are those of the corresponding right-handed squarks. In both cases the index i runs over the colour. For \tilde{q}_i , and the same holds for \tilde{u}_i, \tilde{d}_i ,

$$\tilde{q}_i = -\frac{1}{2} \ln\left(\frac{M_i^2}{Q^2}\right) + 1 - \frac{1}{2r} \left(1 + \frac{(r-1)^2}{r} \ln|r-1|\right) + \frac{1}{2} \theta(r-1) \ln r \quad (13)$$

where $M_i = \max(\tilde{m}_i, |M_3|)$, $r = |M_3|^2/\tilde{m}_i^2$. \tilde{m}_i is the squark soft mass in each case. We have neglected EW mixing effects which have little effect on this formula. This generalizes the result of [79], in which a common squark mass is used, and it is a handy expression to use avoiding the complexities of other calculations. More refined two-loop corrections in terms of several two-point functions are presented in [81, 82]. In that reference it is shown that the two-loop QCD corrections are small.

With the above we end the discussion concerning the treatment of the RGEs by giving an outline of the salient features which have a large impact on our numerical analysis in the CP-violating case. The boundary conditions employed for the couplings at the unification scale were discussed earlier. In our code the soft masses and trilinear scalar masses we treat in the most general case allowing for non-universal boundary conditions for their magnitudes and their phases, as already discussed, in the approximation of neglecting flavour violating interactions in the Lagrangian. Although the setup is to cover the most general case in this respect we shall only discuss particular cases which are of phenomenological and theoretical interest, and focus our attention mainly on models with universal boundary conditions for the magnitudes of the SUSY breaking parameters involved.

4 Running of the CP-violating phases with the energy scale

The case of non-vanishing phases has features that need be further discussed when the two-loop RGEs are used for their evolution. Their values are inputs which can be set at either the unification scale, M_{GUT} , or the average stop scale $Q_{\tilde{t}}$ at which we minimize the one-loop effective potential. In our treatment we work in the basis in which the phase of m_3^2 is put to zero at $Q_{\tilde{t}}$ and the remaining phases we take as inputs at M_{GUT} , as we have already stated. Evidently the phases of all parameters at any other scale are determined by the RGE running. The phase of the μ is very important since it affects the mass spectrum of the charginos, neutralinos and sfermion and it explicitly appears within their corresponding mass matrices. Besides, its phase has a large impact on the radiative corrections of the bottom and top Yukawa couplings and therefore the numerical procedure is very sensitive to its input value. Last, but not least, the phase of μ affects the EDMs of Hg, neutron and electron. A large phase for μ may be in accord with Baryogenesis but its value is severely constrained by the experimental EDM bound of the

electron in mSUGRA models in which only the common gaugino phase and the phase of μ are present.

The RGEs of the parameter μ , the gaugino masses and the electron's trilinear coupling, which also affect the light fermion dipole moments, are as follows

$$\begin{aligned}
\frac{d\mu}{d\ln Q} &= \frac{\mu}{4\pi} (-3\alpha_2 - \frac{3}{5}\alpha_1 + 3h_t^2 + 3h_b^2 + h_\tau^2 + \text{two-loop}) \\
\frac{dM_i}{d\ln Q} &= \beta_i M_i + \text{two-loop}, \quad i = 1, 2, 3 \\
\frac{dA_e}{d\ln Q} &= \frac{1}{4\pi} (-6\alpha_2 M_2 - \frac{18}{5}\alpha_1 M_1 + 6h_b^2 A_b + 2h_\tau^2 A_\tau) + \text{two-loop} \quad . \quad (14)
\end{aligned}$$

For lack of space we do not present the RGEs of the remaining trilinear couplings of the 1st and 2nd generations and we also avoid presenting explicitly the two-loop contributions. The β_i in the RGEs for the gaugino masses are the one loop beta function for the gauge couplings α_i . Since we work in the MFV scenario we have neglected generation mixing terms. In this approximation the trilinear couplings of A_e , as well as the remaining trilinear couplings of the first two generations, do not have any influence on the remaining parameters although they depend on them. In practice this means that one can first solve the RGEs for the rest of the parameters and subsequently determine the trilinear couplings of the first two generations.

The RGEs for the μ parameter has the form $d\mu/d\ln Q = \mu S$ where S is real. Due to this the phase of μ does not get renormalized with the scale. Its value at any scale is the same with its value at M_{GUT} independently of the other phases. The phases of the soft gaugino masses exhibit a slightly different behaviour. Their one-loop RGEs are multiplicative as in the μ case so that they do not get renormalized at this loop order independently of the remaining phases. However this does not hold at the two-loop order. This essentially means that one should expect small renormalization of their phases as we run down from the unification to lower scales and vice versa. Thus, even if their phases at the unification scale are set to zero, small phases are induced at low energies, if the phase of μ or the trilinear couplings are non-vanishing at M_{GUT} . Although small this phenomenon may have dramatic consequences for the EDMs since even small phases may produce large EDMs which are constrained by the data. This effect is more enhanced for the phases of the trilinear couplings which are considerably renormalized since their RGEs are not multiplicative, already at the one-loop, unlike the parameter μ and the gaugino masses. For instance in the case of A_e its one-loop RGE shows a dependence on the gaugino masses and the trilinear couplings of bottom and tau, as is obvious from the third of Eqs. 14. Thus, a non-vanishing phase, for at least one of them, at the unification scale may yield a non-vanishing phase at the EW scale for A_e which in turn affects the EDM of the electron. The same holds for the remaining trilinear couplings. This digression shows how important is to consider the running of the phases as we do in our approach.

As a preview of the impact of the two-loop RGE corrections to the phases, and consequently on EDMs, consider the particularly interesting case arising when the gluino phase ξ_3 is the only non-vanishing phase at M_{GUT} . As is obvious from the above RGEs the phases ξ_1, ξ_2 of M_1, M_2 as well as this of A_e are not affected by ξ_3 at one-loop running. *Therefore at this*

$M_{1/2} = 900, m_0 = 800, A_0 = 500, m_t = 171.4, m_b = 4.25$					
$\xi_3 = 2\pi/10$	$arg(M_1)$	$arg(M_2)$	$arg(A_e)$	θ	$10^{26} \times d_e$
$\tan\beta = 50$	-0.0144	-0.0198	-0.1735	0.0465	+1.0845
$\tan\beta = 10$	-0.0149	-0.0209	-0.0079	0.0006	-0.1654

Table 2: The induced phases, at M_Z , of $M_{1,2}, A_e$, the misalignment angle θ and the value for the electron EDM when only the gluino phase $\xi_3 = \pi/5$ is switched on at the unification scale, for $\tan\beta = 50, 10$ respectively. The inputs (in GeV) are shown on the top of Table. $M_{1/2}, m_0, A_0$ are the magnitudes of the common gaugino and scalar masses and trilinear couplings at M_{GUT} .

loop order the electron EDM bound does not depend on ξ_3 . However at the two-loop order the phases for M_1, M_2, A_e do depend on ξ_3 affecting the EDM, d_e , of the electron. In some cases this dependence may have important consequences inducing corrections to EDMs that are comparable to those induced by the Barr-Zee type two-loop contributions which are known to be sizable for large A and $\tan\beta > 30$. If, for instance, ξ_3 is the only non-vanishing phase switched on at the unification scale the induced phases for M_1, M_2, A_e may result to values for electron's EDM that can even saturate the experimental limits put on d_e . A typical case is shown in Table 2, for $\tan\beta = 50$ and $\tan\beta = 10$ respectively. The remaining inputs are as displayed in Table. Throughout this paper, if not otherwise stated, $M_{1/2}, m_0$ and A_0 will denote the magnitudes of the common soft gaugino and scalar masses and the common trilinear scalar coupling respectively. For $\xi_3 = 2\pi/10$ at M_{GUT} the phases of $M_{1,2}$ at the EW scale are $\sim 10^{-2}$. The phase of A_e is $\phi_{A_e} \sim 10^{-1}(10^{-2})$ for $\tan\beta = 50(10)$. For completeness we also display the value of the calculated misalignment angle θ which also affects EDMs. It is seen that values for d_e which are larger than the experimental limits quoted in literature, $|d_e| < 1.6 \times 10^{-27}$, are induced for these particular inputs. However this is a generic feature valid in a large regions of the $m_0 - M_{1/2}$ plane. In Fig. 1 we display the ratio $|d_e/d_e^{exp}|$ of the predicted electron's edm to its experimental bound as function of the gluino angle ξ_3 , which is assumed to be the only non-vanishing input CP-violating input at M_{GUT} , for two different values of $\tan\beta = 20, 40$. The remaining inputs are displayed in the figure. This ratio should be less than unity for the experimental bound to be observed. A strong dependence on the angle ξ_3 is seen which is absent at the one-loop RGE running. This restricts the allowed ξ_3 values to be in the vicinity of $0, \pm\pi$ for $\tan\beta = 20$. Increasing to $\tan\beta = 40$ the dependence of d_e is still strong, but slightly milder, and the allowed range for ξ_3 gets broadened. In this case one observes that large $\tan\beta$ values allow for non-trivial gluino phases which are welcome since they can be used in order to lower the neutron's edm by using the cancellation mechanism as we shall discuss.

The dependence of the M_1, M_2, A_e phases on ξ_3 may also affect the cancellation mechanism if phases are inputs at the GUT scale. Rotating the phase ξ_1 till d_e becomes vanishingly small, to comply with its experimental bounds, a subsequent rotation of ξ_3 at M_{GUT} , in order to make neutron's EDM small within its experimental limits as prescribed in [20], will shift the initially found ξ_1 invalidating the cancellation between neutralino and chargino contributions in d_e . Certainly this is not the case when this procedure is implemented with phases given at the EW scale. Therefore the determination of cancelling phases in the top-bottom approach poses

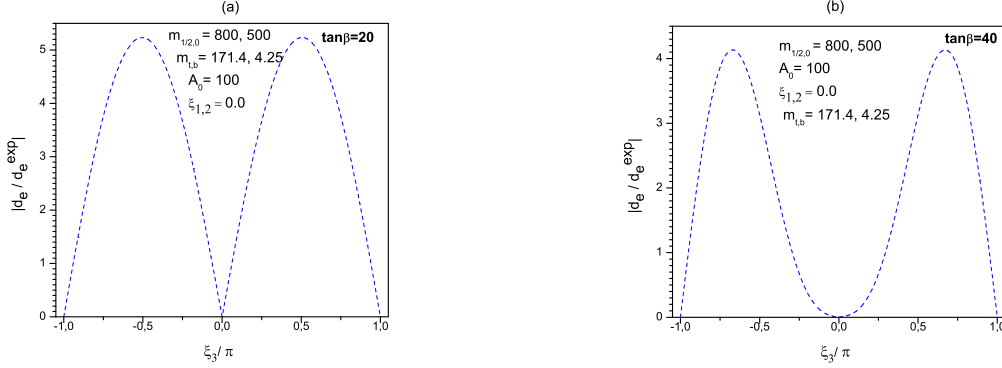


Figure 1: The ratio $|d_e/d_e^{exp}|$ of the predicted electron's edm to its experimental bound as function of the gluino phase ξ_3 , for two different values of $\tan\beta = 20$ (left panel) and $\tan\beta = 40$ (right panel). The remaining inputs are displayed in the figure.

difficulties not encountered in the one-loop RGE running. In addition, even if proper phases are found at M_{GUT} by the cancellation mechanism, so that electron and neutron EDM become small for some particular SUSY inputs, it is difficult to delineate regions by merely rescaling the SUSY parameters as prescribed in [20]. The reason is that due to their RGE running the induced phases at low energies depend on SUSY inputs and a rescaling dislocates the values of the low energy phases by little amounts but enough to make the cancellation invalid. We are therefore arguing that the cancellation mechanism is best suited for a bottom-up approach although it may still be a powerful tool to locate regions compatible with EDMs and all other data when CP-violating phases are switched on as we shall discuss.

The role of the misalignment angle θ to the EDMs should not be passed unnoticed. This is measurable and cannot be rotated away [1,60,61]. Its value enters and affects various physical quantities. The neutralino, chargino, squark and slepton masses depend on this through the combination $arg(\mu) + \theta$ as has been already stated. It also affects the Higgs decays to $b\bar{b}$ enhancing the widths for these decays [60] which has important implications for the cosmologically acceptable regions in which LSP pair annihilation takes place near a Higgs resonance. This mechanism depends sensitively on the corresponding widths. It has also impact on EDMs especially in the large $\tan\beta$ regime. In Fig. 2, for some particular inputs, we display the values of the angle θ and the electron dipole moment, d_e , with and without the inclusion of θ in its calculation. The angle θ takes values from $\sim 10^{-4}$ to $\sim 10^{-2}$ for $\tan\beta$ in the region $5 - 50$. On the left panel the gluino phase has been taken vanishing at the GUT scale and the difference in d_e reaches 50% for $\tan\beta = 50$. On the right panel in addition the gluino phase is switched on and the difference gets much larger. Therefore the misalignment angle produces large effects when $\tan\beta$ is large, which are further augmented if in addition the gluino phase is large at the unification scale. Since θ has large impact on EDMs, in particular regions of the parameter space, it influences the cancellation mechanism as well, in the large $\tan\beta$ region, especially when large values for the gluino phase are required to make neutron's EDM small within its experimental

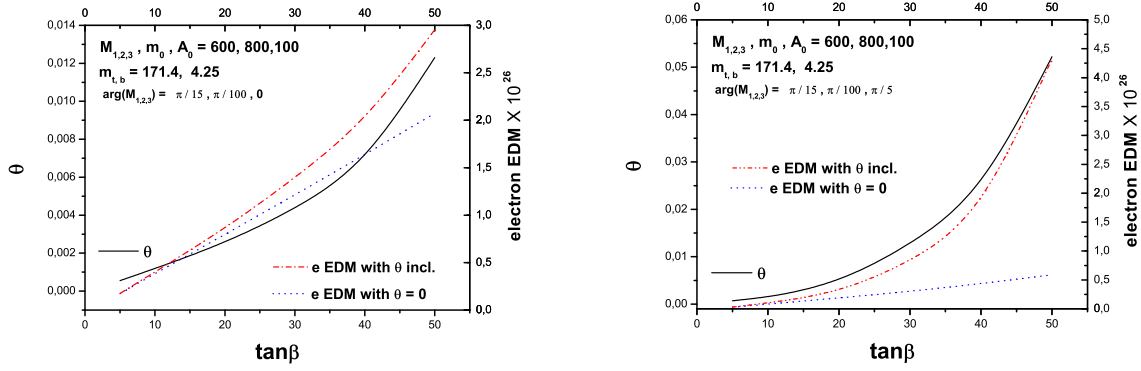


Figure 2: The misalignment angle θ (solid line) and the electron dipole moments, with θ included (dashed-double dotted line) and with θ set to zero (dotted line), for the inputs shown on the figure. Masses are given in GeV and $M_{1,2,3}, m_0, A_0$ refer to the magnitudes of the corresponding parameters. On the left (right) panel the M_3 phase is set to 0 ($\pi/5$).

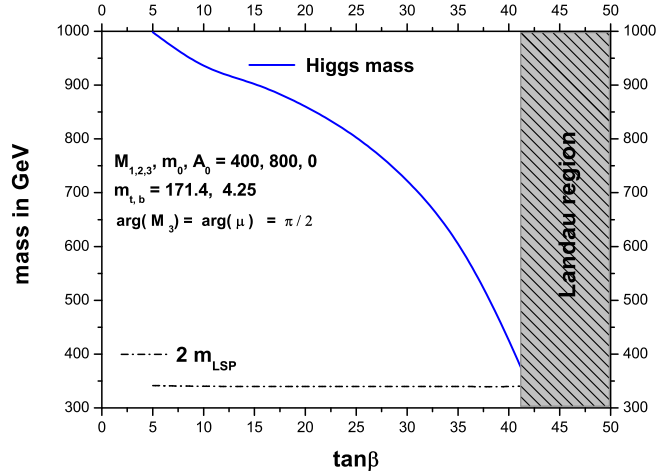


Figure 3: One of the heavy neutral Higgs mass (solid line) and the value of twice the LSP neutralino mass (dash-dotted line) as functions of $\tan\beta$ for the inputs shown in the figure. Above $\tan\beta \simeq 41.0$ a Landau pole is developed.

bounds.

As already stated in this section, the phases of the Higgsino parameter μ and that of the soft gluino mass ξ_3 affect the analysis a great deal. The first, if large, affects the EDM of electron which imposes the stringent constraint on the phase ϕ_μ of μ , while both affect the corrections to the bottom mass especially for large values of $\tan\beta$ having a large impact on the DM relic density. This is clearly seen in Eq. 5 or its more simplified form 6 where the corrections to

bottom mass are encoded in. From Eq. 6 we see that if ϕ_μ, ξ_3 are such that $\cos(\phi_\mu + \xi_3) < 0$, at low energies, these corrections, depending on inputs, can be large and negative, in the large $\tan\beta$ regime. Therefore in view of Eq. 4 they may yield large values for the bottom Yukawa coupling. In this case one should be prepared to encounter the appearance of Landau poles and the top-down approach can not be handled perturbatively. Therefore the link between low energy and GUT scale physics is questioned in this case. This behaviour imposes a severe obstacle when large phases are sought in conjunction with large $\tan\beta$ values which is the requirement for the LSP annihilation through a Higgs resonance. In Fig. 3 we present such a situation for the inputs displayed on the figure. In this figure we observe the evolution of one of the heavy neutral Higgses mass, m_{H_3} , and the double of the LSP neutralino mass, $2 m_{LSP}$, as functions of $\tan\beta$. The Higgs mass tends to $2 m_{LSP}$ as $\tan\beta$ increases and would eventually catch the $2 m_{LSP}$ line signaling approach to a point where LSP pair annihilation through a Higgs resonance dominates the relic density. However it is shown that this is abruptly stopped due to the development of a Landau pole at around $\tan\beta \simeq 41$. This effect, not considered in previous analyses, may exclude particular points in the parameter space and shrink the allowed funnel regions.

5 Cosmologically and EDMs allowed domains

In the previous section we gave an account of the salient features of MFV models when CP is violated. Our principal aim in this section is to explore regions of the parameter space in which the LSP neutralino relic density is within the stringent limits put by WMAP3, satisfying at the same time the EDMs and all available accelerator constraints. We focus our analysis on regions where the LSP neutralinos are paired annihilated through a Higgs resonance which is one of the prominent mechanisms in CP-conserving models, in order to obtain acceptable relic densities, although other regions of interest will be also explored. Regions of the parameter space in which such a process is feasible, when CP is conserved, have the shape of funnels lying on each side of the line on which $2m_{LSP}/M_A$ is unity and this occurs for large values of $\tan\beta$. In the presence of CP violation, and especially for large values of the phases which we are interested in, the shape and the location of the funnels are different due to the impact of the phases on the corrections to bottom mass as has been discussed in the previous section. There are two cases which one should be interested in:

- A. Cases where EDMs are naturally suppressed, without invoking any special mechanism, to lower the values of EDMs to acceptable levels having at the same time some of the phases large. These regions correspond to large $m_0, M_{1/2} > \mathcal{O}(\text{few TeV})$. Certainly the EDMs can be suppressed if all phases are very tiny but this case is not physically interesting.
- B. Cases where EDMs are suppressed due to cancellations among the various contributions. This requires a tuning of the phases at low energies that have a large impact on EDMs.

In general EDM constraints exclude a large portion in the $m_0, M_{1/2}$ plane allowing large values of m_0 or $M_{1/2}$ so that the EDMs are naturally suppressed. Thus, depending on inputs they cut off substantial part, or all, of the cosmologically allowed neutralino and stau coannihilation [83] tale

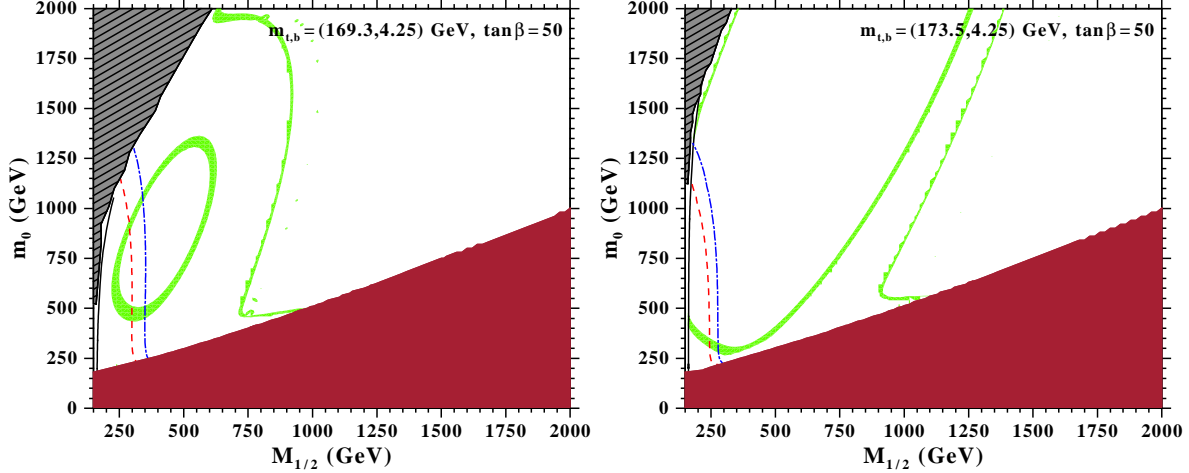


Figure 4: The cosmologically allowed region (shaded light green) for $m_t = 169.3$ GeV (left panel) and $m_t = 173.5$ GeV (right panel), when all the phases are switched off, for $\tan\beta = 50$. The magnitude of the common trilinear scalar coupling is taken $A_0 = 100$ GeV. The remaining inputs are shown on the figure. The solid black line on the left of the figure is the chargino mass bound $m_{\tilde{c}} > 105$ GeV. The red dashed (blue dashed-dotted) line indicates the Higgs mass bound 114 GeV (115 GeV). The hatched area at the left-top designates the no-electroweak symmetry breaking region. At the bottom the shaded region is excluded since there the stau is the LSP.

and focus point region [84] as well. At the same time they cut part of all of the cosmologically allowed region in which neutralinos annihilate through a Higgs resonance. These regions have the shape of funnels, whose location and form is sensitive to the top and bottom masses and may occupy regions allowed by the EDM constraints, if they happen to span large $m_0, M_{1/2}$ values. The sensitivity with the top mass is shown in Fig. 4. On the left panel and for the inputs shown we display the cosmologically allowed region for $m_t = 169.3$ GeV, the lowest allowed by the experimental data for the top mass. On the right panel the same figure is shown with $m_t = 173.5$ GeV which is the upper experimental limit. In both cases all phases are switched off but this behaviour holds in CP-violating cases as well. In the first case the cosmologically allowed regions, which follow the $M_{Higgs}/2m_{LSP} = 1$ curve, are not so peaked and occupy regions characterized by $M_{1/2} < 900$ GeV. Increasing m_t , on the right panel, the location of the line $M_{Higgs}/2m_{LSP}$, which controls the location and the shape of the rapid Higgs annihilation region, turns to the right dragging with it the cosmologically allowed region to higher $M_{1/2}$ becoming more pronounced and extended. This behaviour is due to the sensitivity of the Higgs mass spectrum with m_t . The larger the top mass is the sharper the shape of the funnel, which extends towards large $m_0, M_{1/2}$ values, and larger the possibility of overlapping with EDM allowed regions. For the bottom mass the tendency is rather opposite and it is low values of m_b that favour the formation of sharp cosmologically allowed funnels.

From the previous discussion it becomes evident that regions allowed by both EDM and DM constraints are easier to find for the highest allowed values of the top mass and values of the phases that make the running bottom mass minimum. In previous works [66] the values of the

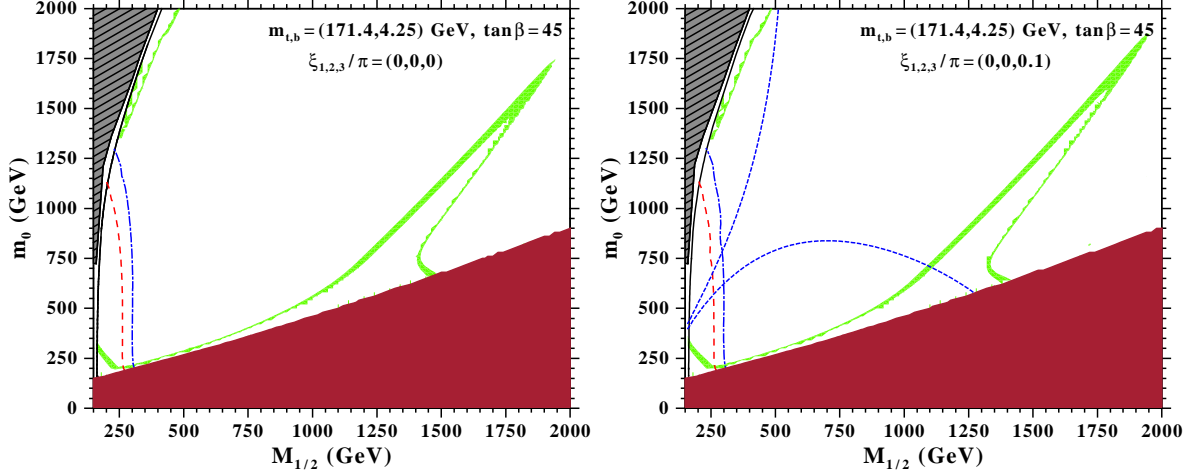


Figure 5: The effect of the gluino phase alone for $\tan \beta = 45$. On the right (left) panel we take $\xi_3 = 0.1\pi$ ($\xi_3 = 0$). The remaining phases are zero and $A_0 = 100$ GeV. On the right panel all displayed region is excluded by neutron and Hg EDM bounds. The allowed region by the electron EDM bound, $d_e = 1.6 \times 10^{-26} e \cdot cm$, lies between the blue short-dashed lines. The rest of the curves and shaded regions are as in Fig. 4.

top quark was taken as large as 178 GeV in agreement with the experimental values quoted at that time. In view of the new experimental values of m_t , according to which m_t is lowered by about ~ 5 GeV, and due to the sensitivity on the top mass of the cosmologically funnels for LSP annihilation through a Higgs resonance, this picture may be distorted. It should be also remarked that in our analysis the situation is different from that encountered in [66] where Yukawa unification is enforced. In that case Yukawa unification entails to a different bottom mass value at each point of the $m_0 - M_{1/2}$ plane and therefore due to the sensitivity on m_b our findings cannot be directly compared to those of [66].

Before embarking on presenting our results we remark that for the calculation of the electric dipole moments and the Higgs masses we use the *FeynHiggs-2.5.1* code, [85]. However since $\langle H_2 \rangle$ is not real, in order to implement the effect of the misalignment angle θ , one has to replace the phase ϕ_μ of μ by $\phi_\mu + \theta$. For the electric dipole moments of the known species the correctness of this we have also checked numerically by comparing the outputs of our numerical routines against to those returned by *FeynHiggs*. For the Higgs masses, in all cases studied, the Higgs mass spectrum obtained was close to that obtained by using the effective potential, with an accuracy 2 – 5%. The latter is known to be less accurate, since the wave function renormalization effects are not counted for. Therefore in this work we use the Higgs masses as returned by *FeynHiggs* and this comparison serves as a further check of the correctness of our treatment. Concerning the experimental limits put on Higgs masses, the ratio $\xi^2 = (g_{hZZ}/g_{hZZ}^{SM})^2$ of the light Higgs boson h coupling to Z , g_{hZZ} , to that of the corresponding SM coupling g_{hZZ}^{SM} is considered for each case studied. This was found to be very close to unity, that is the light Higgs acts like a SM Higgs boson, and therefore the *LEP2* limit $m_h > 114.5$ GeV applies. This is expected in the constrained model studied in this work since we are within the decoupling region.

In case **A** in order to locate regions compatible with all available data the funnel must be extended towards high $m_0, M_{1/2}$ entering regions in which EDMs are naturally suppressed. However, we have found that this cannot occur since EDM bounds require very high $m_0, M_{1/2}$ not overlapping with the cosmologically allowed funnel regions, unless, the CP-violating phases are very small. In order to conceive the picture, and for demonstrating the importance of a non-zero gluino phase, on the left panel of Fig. 5 we display the cosmologically allowed regions, having the shape of funnels, when CP-violating phases are absent. The magnitude of the common trilinear scalar coupling is taken $A_0 = 100$ GeV. The remaining inputs are shown on the figure. The hatched area on the left is not allowed due to the absence of EW symmetry breaking there. The solid black line on the left of the figure is the chargino mass bound $m_{\tilde{c}} > 105$ GeV. The dashed line (in red) sets the Higgs mass boundary line $m_{Higgs} > 114$ GeV, while to the right of it the dashed-dotted line (in blue) designates the bound on the Higgs mass reported by D0 [69], $m_{Higgs} > 115$ GeV. On the right panel for the same inputs we switch on the gluino phase $\xi_3 = 0.1 \pi$. The funnel is slightly deformed with its top end approaching the point $m_0 = M_{1/2} = 2000$ GeV. However all displayed region is excluded by neutron and Hg EDM bounds and it is not of physical relevance. The electron EDM, d_e , is also affected and allows the region confined between the short-dashed lines (in blue). This figure demonstrates in a clear way the impact of the gluino phase on d_e by the two-loop RGE running of the phases, as discussed in the previous section.

The other option opened, case **B**, is to implement the cancellation mechanism according to which phases are chosen so that the various contributions to EDM cancel each other. This option does not require high values for $m_0, M_{1/2}$. Starting for such a point in the parameter space one can draw trajectories, by merely rescaling the values of m_0 and $M_{1/2}$, in which EDMs are in agreement with the experimental bounds put on them [20]. These trajectories may eventually overlap with the cosmologically allowed portions and thus delineate regions allowed by both EDM and cosmological constraints. In the previous section we discussed that this is rather difficult to be accomplished in the top-down approach due to the two-loop running of the phases and the interplay among these. Certainly the phases can be tuned at the EW scale to cancel separate contributions in electron and neutron dipole moments. If such values are obtained at the EW scale, when one is subsequently trying to find extended regions by rescaling as $m_0, M_{1/2} \rightarrow \lambda m_0, \lambda M_{1/2}$, the RGE evolution of these phases at the GUT scale yields values that depend on the parameter λ . Therefore their values at M_{GUT} are fine tuned since they are different for different pairs of $m_0, M_{1/2}$ that are related by a rescaling factor. Therefore in the top-down approach it is difficult to find extended regions in the $m_0, M_{1/2}$ plane by just rescaling the supersymmetry breaking parameters as prescribed before.

In our approach, for given inputs for the supersymmetry breaking parameters, we prefer to implement this mechanism by rotating the input phases $\xi_{1,2,3}$ at the GUT scale until an acceptable point is found respecting the EDM limits on electron and neutron. Subsequently keeping fixed the values of the phases we vary $m_0, M_{1/2}$ to delineate regions compatible with all available data. Alternatively one can vary the phases around the values for which small EDMs for the electron and neutron were obtained, keeping the remaining inputs fixed, in order

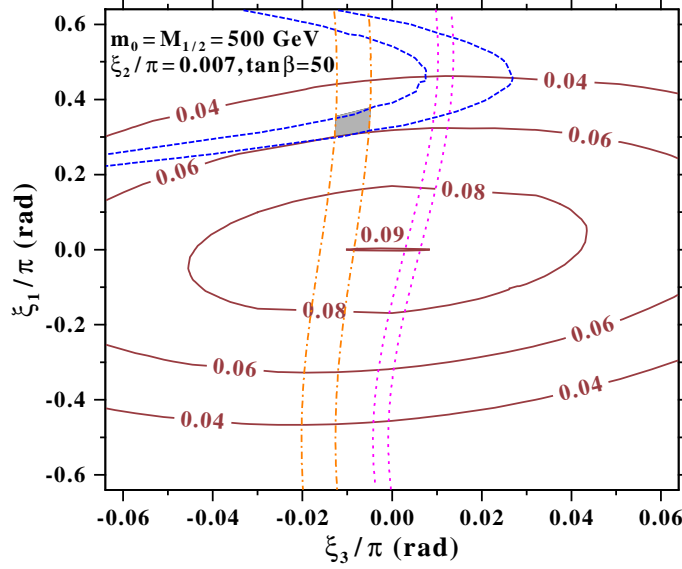


Figure 6: The EDMs and relic density contours for $m_0 = M_{1/2} = 500$ GeV, $A_0 = 100$, $\tan \beta = 50$, and $\xi_2 = 0.007\pi$ on the (ξ_3, ξ_1) plane. The remaining phases are zero at the GUT scale. The blue dashed (orange long dashed-dotted) curves designate the d_e (d_n) acceptable region. The allowed region by d_{Hg} is this between the magenta dotted lines, which does not overlap with the grey region allowed by electron and neutron EDMs. The contours of constant neutralino relic density are shown as solid elliptical curves. The region favoured by WMAP3 data is located in the centre of the figure not overlapping with any of the the EDM allowed domains.

to locate regions in which large phases are obtained satisfying all experimental bounds. The role of the phase ξ_3 is vital in this approach. For fixed ξ_2 one varies ξ_1 until the electron EDM d_e is small, by cancelling chargino against neutralino contributions. Subsequently ξ_3 is rotated until the neutron's EDM, d_n , is made small.

This is the prescription followed in [20] to make both d_e and d_n lie within their experimental limits. However as discussed in the previous section due to the two-loop RGE dependence of d_e on ξ_3 the cancellation in d_e may be lost and therefore ξ_1 need be re-rotated. It should be remarked that for large $\tan \beta$ the two-loop contributions are important and cannot be ignored. In those cases therefore we apply this recipe by taking into account the appearance of two-loop contributions, as well as additional contributions from other sources, such as chromoelectric dipole and gluonic dimension-6 operators, which may be important. Therefore following this procedure one may be able to find points in the $\xi_{1,2,3}$ parameter space yielding small d_e, d_n . In this case however the Hg dipole moment is not guaranteed to be within its experimental limits. Besides, since the cosmologically allowed regions depend on these phases, even if we start from a point on which the relic density is acceptable and implement the cancellation mechanism, we do not necessarily end up with phases that respect the cosmological bounds put on the relic densities. Such a situation is depicted in Fig. 6. For the given inputs the phases $\xi_{1,2,3}$ are rotated until the electron's and neutron's EDMs are within their experimental limits. This point

corresponds to $\xi_2 = 0.007 \pi$ and values of $\xi_{1,3}$ located at the centre of the small grey shaded region shown in the figure. This grey region is the overlap of the two stripes, one between the dashed lines, which designates the d_e acceptable region, and the other between the dotted-dashed lines which designates the region allowed by the neutron EDM bounds. Starting from this particular $\xi_{1,2,3}$ point, and keeping ξ_2 fixed, we have plotted in the $\xi_{1,3}$ plane the allowed domains by EDM and relic densities. The allowed region by the Hg dipole moment is confined between the dotted lines (in magenta) which, as one can see, does not overlap with the grey region allowed by electron and neutron EDMs. In this figure it is also seen how the phases are fine tuned, especially ξ_3 , to achieve acceptable EDMs for the electron and neutron in the sense that only in a small region both d_e and d_n can be within their experimental bounds. On the same figure the contours of constant neutralino relic density are shown as solid elliptical curves. In the example shown, one observes that the location of the region favoured by WMAP3 data occupies only a small portion at the centre of the figure at which $\xi_{1,2} \simeq 0.0$ not overlapping with the EDM allowed domains. This figure represents a rather typical example of the difficulty one encounters to reconcile both EDMs and cosmological bounds.

In Fig. 7 we have taken moderate values $m_0 = 500$ GeV, $M_{1/2} = 480$ GeV, $A_0 = 100$ GeV. and large $\tan \beta = 50$. The masses of the top and bottom are $m_{t,b} = 171.4, 4.25$ GeV. The figure is constructed from one million random points in the $\xi_{1,2,3}$ parameter space. All other phases are assumed zero at the unification scale. Initially a particular point, $\xi_{1,2,3} = -0.072\pi, 0.953\pi, 0.047\pi$ is found by tuning the phases, in the way described earlier, satisfying all EDM bounds including in this case the EDM constraints from Hg atoms as well. The random sample is chosen to include this particular point. In Fig. 7 we classify these points in the planes $\xi_{1,3}$ (left panel) and $\xi_{2,3}$ (right panel) according on what bounds each point satisfies. Light grey squares, forming the dense light grey region (region-1), includes points that satisfy only the Higgs and chargino mass bounds. The subset of these, shown as dark grey region (region-2), includes points that in addition they satisfy the upper observational limit for the relic density, i.e. $\Omega_{\tilde{\chi}} h_0^2 < 0.117$ but they do not necessarily fall within the region dictated by the WMAP3 region. Their subset, marked as triangles (region-3), are within the 2σ WMAP3 limits for CDM, $0.089 < \Omega_{\tilde{\chi}} h_0^2 < 0.117$. For the rest $\Omega_{\tilde{\chi}} h_0^2 < 0.089$ and therefore they are of relevance if additional components, except the LSP neutralino, contribute to the total DM density.

The points shown as coloured-filled diamonds satisfy the electron and neutron EDM bounds. Of those only their subset filled with different colour (red) satisfy, in addition, the Hg EDM bounds. If any of these points falls on regions-1,2 or 3, defined before, then in addition it satisfies the corresponding bounds designating this particular region. One observes that irrespectively of the cosmological, and other accelerator data, the EDM bounds by themselves are hard to satisfy for moderate $m_0, M_{1/2}$. Despite the fact that a particular point was found which respects all three EDM bounds, the random sample of one million points in the $\xi_{1,2,3}$ space leaves only a few that observe the EDM limits for electron and neutron and even fewer that satisfy all three EDM constraints. This demonstrates that the values of the phases must be fine tuned to comply with experimental data of electric dipole moments. In the examples shown none of the diamond points satisfy the WMAP3 cosmological constraints. In fact for these points the

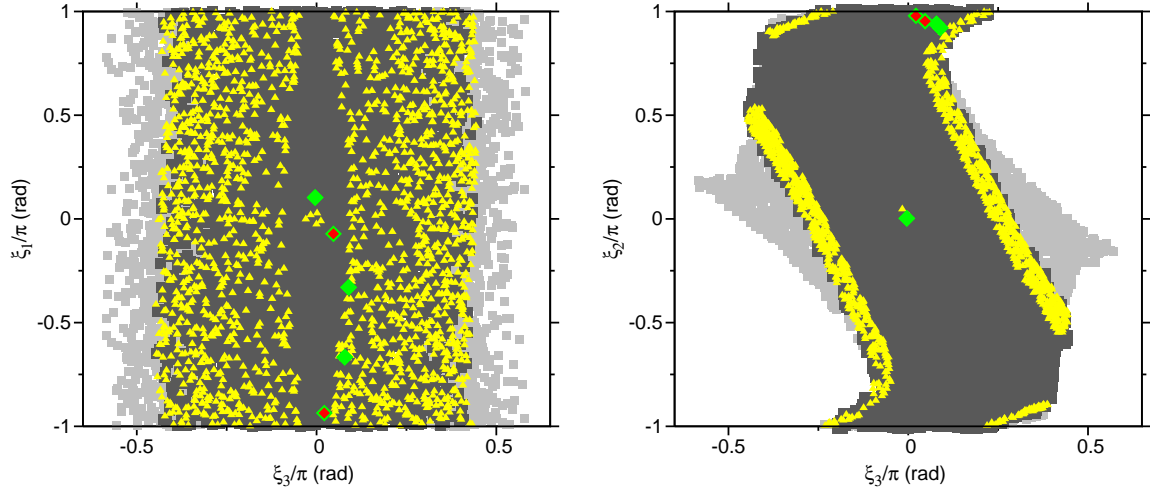


Figure 7: Scatter plots in ξ_3, ξ_1 (left panel) and ξ_3, ξ_2 (right panel) plane, based on a random sample of the gaugino phases $\xi_{1,2,3}$ for fixed $m_0 = 500$ GeV, $M_{1/2} = 480$ GeV, $A_0 = 100$ GeV and $\tan \beta = 50$. The remaining phases at the unification scale are taken zero. The light grey squares represent points that satisfy the mass bounds for the light Higgs boson and other SUSY particles. The dark grey region is formed from points that in addition they satisfy the upper WMAP3 bound for the relic density $\Omega_{\tilde{\chi}} h_0^2 < 0.117$. The yellow triangles represent their subset falling within the WMAP3 region, $0.089 < \Omega_{\tilde{\chi}} h_0^2 < 0.117$. The one-colour (green) diamonds satisfy the electron and neutron EDM bounds, while those filled with different colour (red), satisfy, in addition, the Hg EDM bounds. Depending on which region they lie on, they may observe the bounds put by WMAP3.

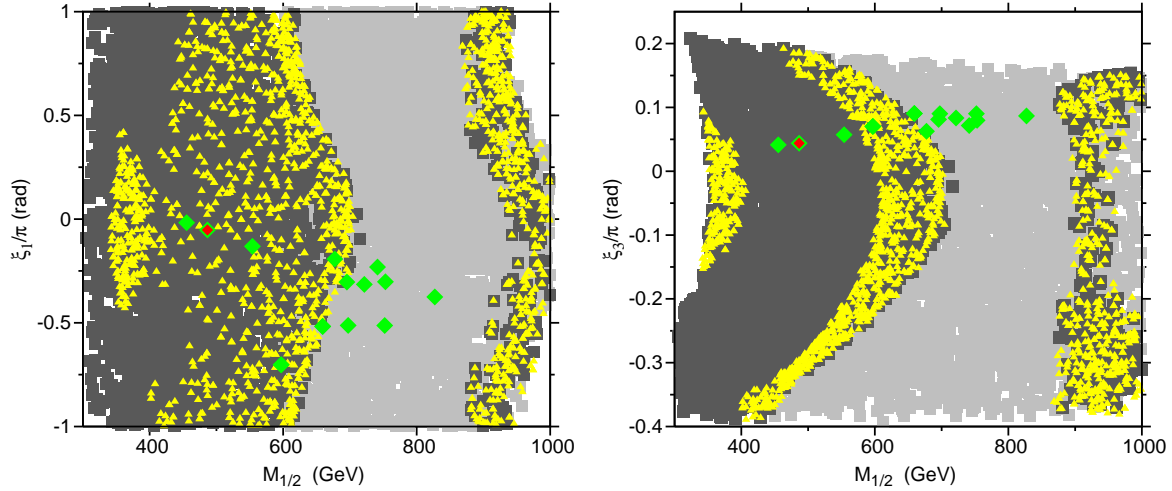


Figure 8: Scatter plots in $\xi_1, M_{1/2}$ (left panel) and $\xi_3, M_{1/2}$ (right panel) plane, for a random sample with ξ_2 fixed and random values for $\xi_{1,3}$ and $M_{1/2}$. The notation is as in Fig. 7.

predicted neutralino relic density is below the limits put by WMAP3 and therefore additional DM candidates must exist to fill the deficit.

In Fig. 8, with the same starting values for the phases $\xi_{1,2,3}$ and the parameters m_0 , $M_{1/2}$, A_0 , $\tan \beta$, for which agreement with all EDM bounds are obeyed, we keep ξ_2 fixed and generate a random sample of one million points for $\xi_{1,3}$ and $M_{1/2}$. The sample includes the starting values for $\xi_{1,3}, M_{1/2}$. In $\xi_1, M_{1/2}$ (left panel) and $\xi_3, M_{1/2}$ (right panel) planes, the points satisfying the particular criteria as described in Fig. 7 are displayed. The notation is as in Fig. 7. The points satisfying the electron and neutron EDM bounds are few, and only one satisfies all three EDM bounds. In the case considered a few of these points overlap with the region-3 (yellow triangles) and therefore for these all available data are obeyed, with the exception of the Hg EDM bound. The limited number of points satisfying the EDM bounds, in this case too, it indicates that the phases must be fine tuned to agree with experimental data.

The Hg EDM bound, in general, poses a severe obstacle in obtaining agreement with cosmological data. However by tuning appropriately the gaugino phases there are cases where agreement with all EDMs is obtained at a particular point $m_0, M_{1/2}, A_0$ of the parameter space. Then by varying $m_0, M_{1/2}$ there is a chance that one succeeds in obtaining cosmologically and EDM allowed regions which overlap. The chance of obtaining this is increased if one considers funnel regions of rapid neutralino annihilation via a Higgs resonance, which occupy extended regions in the parameter space. In figures 9 and 10 we display cases for low and large $\tan \beta$. The values for the phases $\xi_{1,2,3}$, in each figure, are fine tuned for specific $m_0, M_{1/2}$, around 600 GeV, in order to obtain agreement with all three EDMs, d_e , d_n , d_{Hg} , for the electron, neutron and Hg respectively. We have taken $A_0 = 100$ GeV and the phase of μ is taken vanishing. All other inputs are shown on the figures. The dashed lines (in blue) delineate the boundaries of d_e , the dotted lines (in magenta) those of d_{Hg} and the dotted-dashed lines (in orange) those of d_n . If only one boundary line is shown it simply means the other one lies outside the displayed $m_0, M_{1/2}$ range. The allowed by EDM constraints regions are between the boundaries in each case. In all cases displayed there are regions where all electric dipole bounds are simultaneously satisfied. Also shown are the Higgs line 114.0 GeV, long-dashed (red), and the line 115.0 GeV, long dashed-dotted (in blue), lying on the left almost vertical to the $M_{1/2}$ axis. Their upper ends touch the no-electroweak symmetry breaking region, designated as a hatched area. At the bottom the triangle-shaped shaded region is excluded since there the stau is lighter than any of the neutralinos. The $2 - \sigma$ cosmologically allowed WMAP3 regions are shown as shaded contours (in light green).

On the left panel of Fig. 9 the value of $\tan \beta = 10$ is small and the cosmologically allowed regions are not so extended. Although for the specific values of the gaugino phases there are large portions of the parameter space compatible with all EDMs, the overlap of these regions with the regions allowed by the WMAP3 data extend to large values of $m_0 > 5.0$ TeV, not shown in the figure, along the focus point region [84]. On the right panel of the same figure the value of $\tan \beta = 30$ is considerably larger and the cosmologically allowed domains have a larger overlap with the regions allowed by EDMs. In this case there is a region in which all data are satisfied for $m_0 \sim 1$ TeV and $M_{1/2} > 2.2$ TeV due to the fact that the allowed by d_e domain is enlarged, allowing for smaller $M_{1/2}$ values, which includes part of a funnel that starts being formed. This is located on the right of the figure, just above the shaded region which is excluded

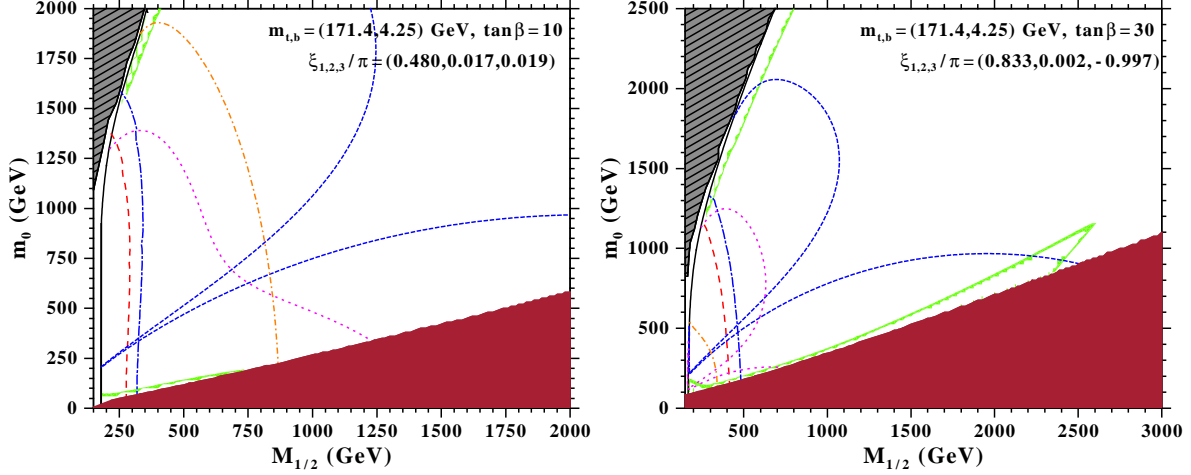


Figure 9: The $m_0, M_{1/2}$ parameter space for non zero gaugino phases, with values shown on the figures. $A_0 = 100$ GeV and the phase of μ is taken vanishing. The dashed lines (in blue) delineate the boundaries of d_e , the dotted lines (in magenta) those of d_{Hg} and the dotted-dashed lines (in orange) those of d_n . If only one boundary line is shown it means the other one lies outside the displayed $m_0, M_{1/2}$ range. The allowed by EDM constraints regions are between the boundaries in each case. The rest of curves and shaded regions are as in Fig. 5.

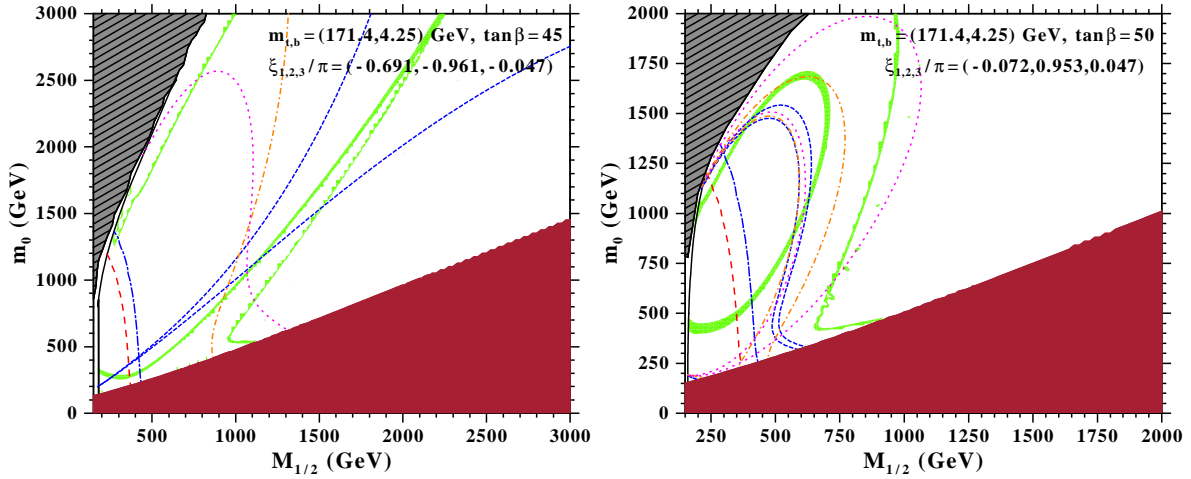


Figure 10: As in Fig. 9 for different values of $\tan\beta$ and the gaugino phases.

since there the stau is the LSP. Due to the heaviness of $M_{1/2}$ this is outside the reach of LHC. As in the left panel case there is also a focus point region, acceptable by all data, starting now from smaller values of $m_0 > 2.1$ TeV, which tracks the border of the no-electroweak breaking region. Part of it includes points with $M_{1/2} < 800$ GeV being therefore accessible to LHC.

Notice that the values of the phases for the right panel are different from those of the case displayed on the left. Due to the fine tuning of the phases chosen increasing the value of $\tan\beta$ from 10 to 30 in the left panel we do not get a picture resembling the one we display on the right panel.

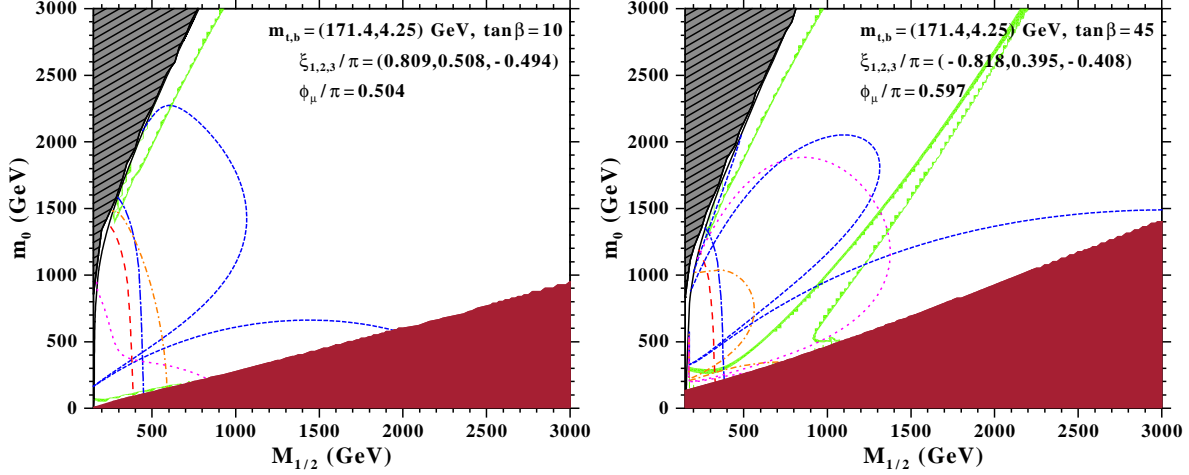


Figure 11: As in Fig. 9, with a non-vanishing phase of μ and values of the gaugino phases and $\tan\beta$ shown in the panels.

In Fig. 10, for different sets of the gaugino phases and large values of $\tan\beta$, we display regions that are allowed by all data. Again the phases have been fine-tuned and are different for each case shown in the two panels. On the left panel the value of $\tan\beta$ is large, $\tan\beta = 45$, and the cosmologically allowed domains are funnel-shaped, extended diagonally towards high m_0 and $M_{1/2}$ values, $m_0 \simeq 3.0$ TeV, $M_{1/2} \simeq 2.2$ TeV. At the same time the acceptable EDM domains are also extended having a large overlap with the cosmologically allowed region. In this particular case there is a large portion of the parameter space for $m_0, M_{1/2} > 1.3$ TeV in which all experimental data are satisfied. A small part of this region is within the reach of LHC. The conclusion from this is that by tuning the gaugino phases there can be found extended regions in the parameter space in which rapid neutralino annihilation through a Higgs resonance can coexist with regions allowed by the stringent constraints imposed by the electric dipole moments. On the right panel the value of $\tan\beta = 50$ is larger and it also allows for the formation of rather extended cosmologically allowed regions which are almost funnel-shaped, but not so peaked as the case considered previously. The boundaries of EDMs in the case shown lie within the range $m_0 < 2.0$ TeV, $M_{1/2} < 1.0$ TeV and one observes that EDM and cosmologically allowed domains again overlap. The overlapping regions are not so extended however, as in the case considered previously. In the case shown it is only a small region centered around the point $m_0, M_{1/2} = 900, 600$ GeV. One observes that larger values of $\tan\beta$, unlike the CP-conserving case, do not always correspond to funnels spanning the highest $m_{0,1/2}$ regions. This is due to the sensitivity of the bottom mass, and hence the funnel regions, with the CP-violating phases. As an effect cosmologically allowed funnel-shaped regions can appear for smaller values of $\tan\beta$, as compared with the CP-conserving case, and can coexist with EDM allowed domains.

In the previous analysis the μ phase has been put to zero but one can also seek for cases where large values of this phase are allowed. This is forbidden in cases where the gaugino phases are switched off. In mSUGRA models, in which the common phase of the trilinear coupling and the μ phase are the only allowed supersymmetric CP-violating sources, it is known that the

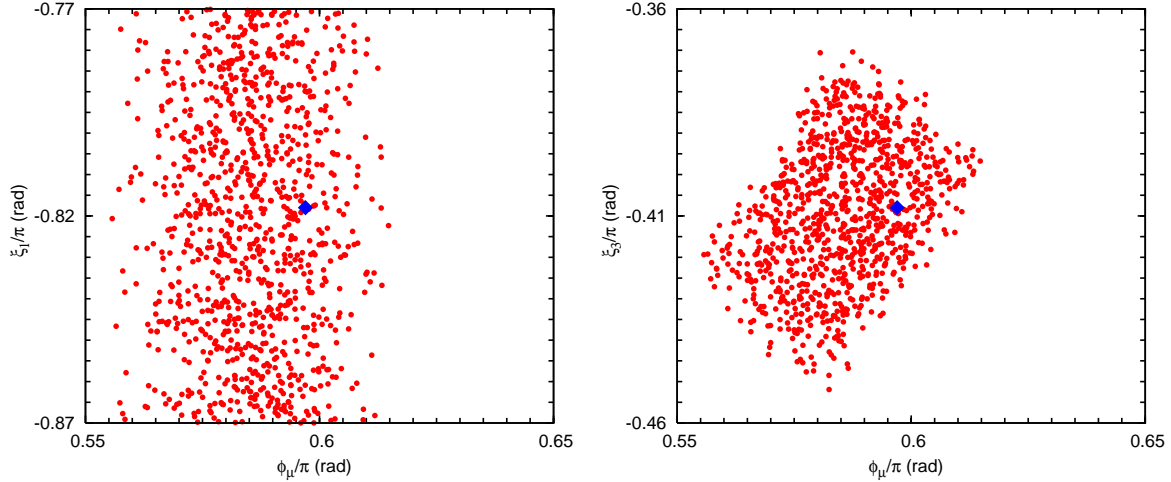


Figure 12: Scatter plots based on a random sample with $m_0 = 2000$ GeV, $M_{1/2} = 1720$ GeV, $A_0 = 100$ GeV, $\tan \beta = 45$ and the phases in the region $-0.87 < \xi_1/\pi < -0.77$, $0.34 < \xi_2/\pi < 0.44$, $-0.46 < \xi_3/\pi < -0.36$ and $0.55 < \phi_\mu/\pi < 0.65$. The dots (in red) are points of the random sample that satisfy all the EDM and cosmological constraints. The (blue) diamond marks the values of the phases used in the right panel of Fig. 11.

phase of μ is tightly constrained by the EDM data, especially by this of the electron. However when one allows for the presence of different gaugino phases the situation is altered and this restriction is relaxed. In Fig. 11 we display a case where ϕ_μ is non-vanishing and large. On the left panel a case with $\tan \beta = 10$ is shown. On the right panel $\tan \beta = 45$. The value of A_0 is $A_0 = 100$ GeV. In both cases the phase of μ is non-vanishing and there are regions compatible with EDMs, cosmological data, as well as all other accelerator data. On the left panel only the focus point region is compatible with all data, while on the right panel both focus point region and the cosmologically allowed funnels are allowed. Both regions include points accessible to LHC, which are larger as compared to the cases considered previously.

Note that the values of $\arg(\mu M_{1,2})$ at M_{GUT} are sizable, $\mathcal{O}(0.1 \pi)$. Due to absence of renormalization of the μ phase with the energy scale and the small renormalization of the gaugino phases, which at one-loop are independent of the SUSY inputs at M_{GUT} , these quantities retain almost the same values at the EW scale M_Z , for every point in the $m_0, M_{1/2}$ plane. The difference of their values at M_Z from those at M_{GUT} is at per mille level which is very small and important only for EDMs. As stated in the introduction these combinations of phases set the measure of sufficient Higgsino and gaugino driven Baryogenesis at the EW phase transition. On these grounds and in conjunction with the fact that the magnitude of μ is comparable to that of $M_{1,2}$ in a large region of the allowed parameter space, displayed in this figure, these regions may be also compatible with these Baryogenesis mechanisms [49–51].

In order to show how sensitive the selected regions are to variations of the phases, which were chosen to suppress the EDMs via the cancellation mechanism, we pick a particular point located in the allowed funnel region on the left panel of Fig. 11. Then by varying the phases $\xi_{1,2,3}$ and ϕ_μ around the values displayed in this figure, we produce a random sample consisting

of 100,000 points. The scatter plots displayed in Fig. 12, are based on this random sample with $m_0 = 2000$ GeV, $M_{1/2} = 1720$ GeV, $A_0 = 100$ GeV, $\tan\beta = 45$ and phases in the region $-0.87 < \xi_1/\pi < -0.77$, $0.34 < \xi_2/\pi < 0.44$, $-0.46 < \xi_3/\pi < -0.36$ and $0.55 < \phi_\mu/\pi < 0.65$. The scattered dots (in red) represent the random points that satisfy all the EDM bounds and the WMAP3 bound on the neutralino relic density. The (blue) diamond in the center of each panel, marks the point corresponding to the values of phases on the right panel of Fig. 11. One can see that the allowed variations on ϕ_μ and ξ_3 are of the order of $\sim 0.05\pi$ rad. The same applies to the phase ξ_2 as well. On the other hand, the range of the values of the phase ξ_1 , that are compatible with the EDM and cosmological constraints, appears to be much broader. Therefore, in the large $\tan\beta$ regime, the amount of tuning required to locate extended cosmological funnels that are also compatible with the EDM bounds, is of the order of 0.01π rad for $\xi_{2,3}$ and ϕ_μ and 0.1π rad for ξ_1 . In the displayed results the phases of the trilinear couplings at the GUT scale are taken zero. However we have checked numerically that variations on them of the order 0.1π rad do not destabilize the cancellation mechanism for the EDMs and therefore the fine tuning of these phases is less restrictive.

6 Conclusions

We have considered supersymmetric models in the presence of CP-violating sources residing in the Higgsino-mixing mass term and SUSY breaking soft parameters. In the simple, mSUGRA based, versions of such models, that have been extensively studied in the past, there are two independent phases at the unification scale usually chosen to be the phase of the Higgsino mixing parameter μ , ϕ_μ , and the phase of the common trilinear coupling A_0 , ϕ_A . The application of the EDM and cosmological bounds constrains the phase of μ to be $\phi_\mu/\pi \lesssim 0.01$ rad, whose smallness poses severe obstacles in certain Baryogenesis mechanisms, while ϕ_A remains practically unconstrained and can be at least ten times larger.

In our study we have used the revised top mass, whose central value is $m_t = 171.4$ GeV, and scan the parameter space allowing for non-universal boundary conditions for the phases at the GUT scale. Such models are described by thirteen CP-violating phases, residing in the gaugino mass terms, the trilinear scalar couplings and the μ parameter, one of which can be rotated away. An additional phase which misaligns the VEVs of the Higgs doublets is determined from the minimization conditions and affects the analysis. We follow a top-bottom approach according to which the low energy values of all parameters involved, including their magnitudes and phases, are determined from their values at the unification scale after running of the renormalization group equations. In such an analysis we showed that the two-loop running of the CP-violating phases induces important corrections to the electric dipole moments of the known species, which are absent in the one-loop running analysis. This results to further constraints of the allowed parameter space. Important corrections to EDMs are also induced by the one-loop misalignment angle of the Higgs vacuum expectation values which are augmented for large $\tan\beta$ and in the presence of a non-vanishing gluino phase.

The role of the gaugino phases is particularly important allowing for suppression of electric dipole moments if they are fine tuned at the unification scale. By tuning appropriately the

gaugino phases $\xi_{1,2,3}$ and the phase ϕ_μ of μ at the unification scale, there can be found regions in the parameter space, along the focus point and neutralino pair annihilation through a Higgs resonance, which are permitted by dark matter WMAP3 cosmological constraints, and are also compatible with the electric dipole moment limits and all accelerator data.

This can be accomplished for large values for the phases of the gaugino masses and the μ parameter, of the order of the $\mathcal{O}(1) \pi$ rad, which are however fine-tuned. The phases $\xi_{2,3}$ and ϕ_μ need to be adjusted at the 0.01π rad level, while the adjustment of ξ_1 is by an order of magnitude less restrictive. The phases of the trilinear scalar couplings although they play a key role for EDMs are not fine tuned when the magnitude of the trilinear coupling is small. The role of the gluino phase is important in this analysis. It can be used, by implementing the cancellation mechanism, to make neutron's electric dipole moment small, and in addition it allows for a large non-vanishing phase for μ . Large values of μ and gaugino phases are needed in certain electroweak Baryogenesis mechanisms. Higgsino and gaugino driven Baryogenesis requires the magnitude of μ to be comparable to the gaugino masses which can be fulfilled in the major portion of the parameter space in the constrained models considered in this work.

Since the suppression of the EDM is feasible for small and intermediate values of the SUSY breaking scale, there are regions in the parameter space which are within the reach of the forthcoming LHC experiments.

Acknowledgments

The work of M.A. and A.B.L. was supported by funds made available by the European Social Fund (75%) and National (Greek) Resources (25%) – EPEAEK B – PYTHAGORAS. They acknowledge also support from the Special Research Account of the University of Athens. The work of V.C.S. was supported by Marie Curie Excellence grant MEXT-CT-2004-014297 and Marie Curie International Reintegration grant “SUSYDM-PHEN”, MIRG-CT-2007-203189. In addition, A.B.L. and V.C.S. acknowledge support by the Research Training Network “HEP-TOOLS”, MRTN-CT-2006-035505.

1 Appendix

In this section we present the basic expressions and conventions used in this work so that a direct comparison with other works and different notations is made possible. The supersymmetric part of the Lagrangian is specified by a superpotential given by

$$\mathcal{W} = h_t Q^T \epsilon H_2 U^c + h_b Q^T \epsilon H_1 D^c + h_\tau L^T \epsilon H_2 E^c + \mu H_1^T \epsilon H_2, \quad (\text{A.1})$$

where the elements of the antisymmetric 2×2 matrix ϵ are given by $\epsilon_{12} = -\epsilon_{21} = 1$. In the superpotential above we have only shown the dominant Yukawa terms of the third generation and we do not allow for flavour mixings. According to this the Yukawa couplings of the left,

right handed top and bottom multiplets are

$$\mathcal{W} = h_t H_2^0 U U^c - h_b H_1^0 D D^c \quad .$$

The scalar soft part of the Lagrangian is given by

$$\begin{aligned} \mathcal{L}_{scalar} = & - \sum_i m_i^2 |\phi_i|^2 \\ & - (A_t h_t Q^T \epsilon H_2 U^c + A_b h_b Q^T \epsilon H_1 D^c + A_\tau h_\tau L^T \epsilon H_2 E^c + h.c.) \\ & - (m_3^2 H_1^T \epsilon H_2 + h.c.) , \end{aligned} \quad (\text{A.2})$$

where the index i in the sum in the equation above runs over all scalar fields and all fields appearing denote scalar parts of the supermultiplets involved.

The gaugino fields soft mass terms are given by

$$\mathcal{L}_{gaugino} = -\frac{1}{2} (M_1 \tilde{B} \tilde{B} + M_2 \tilde{W}^{(i)} \tilde{W}^{(i)} + M_3 \tilde{G} \tilde{G} + h.c.) \quad (\text{A.3})$$

In this equation \tilde{B} , $\tilde{W}^{(i)}$, \tilde{G} are the gauge fermions corresponding to the $U(1)$, $SU(2)$, and $SU(3)$ gauge groups. Our notation is that of Ellis and Zwirner [86] with the signs of the gaugino masses and that of the bottom and tau Yukawa couplings reverted. The one-loop RGEs found in that reference coincide with ours if the signs of the gaugino masses are flipped. RGEs of course are insensitive to the Yukawa sign convention.

The two-loop renormalization group equations (RGEs) in the general case, including supersymmetric CP violations, can be read from [72] and [73]. In [72] the soft SUSY breaking part of the Lagrangian is written as

$$\mathcal{L} = -\frac{1}{6} h^{ijk} \phi_i \phi_j \phi_k - \frac{1}{2} b^{ij} \phi_i \phi_j - \frac{1}{2} (m^2)_i^j \phi_i \phi_j^* - \frac{1}{2} M_{(a)} \lambda_a \lambda_a + h.c. \quad (\text{A.4})$$

Keeping only flavour diagonal mass terms for the scalars ϕ_i , as we have assumed throughout, the mass terms become

$$\mathcal{L} = -\text{Re}(m^2)_i^i |\phi_i|^2 .$$

From Eq. (1) we observe that the imaginary parts of $(m^2)_i^i$ do not appear in the Lagrangian. Besides it is easy to see that the RGEs of the quantities appearing in the Lagrangian do not depend on the imaginary parts of $(m^2)_i^i$. Therefore they do not affect the physical quantities and can be taken anything.

For the two-loop RGEs, those of the trilinear couplings $A_{t,b,\tau}$ are found if one replaces h_{ijk} and the Yukawas couplings Y_{ijk} in the RGEs found in [72] by $h \equiv -A \cdot Y$, where we have suppressed the flavour indices, and identifying the gaugino masses used in that reference with ours. The one-loop parts of the RGEs we get with such a replacement coincide with our one-loop RGEs for the $A_{t,b,\tau}$ which are identical, modulo the sign difference in the gaugino masses as mentioned before, with reference [86]. Note that the same would not have happened have we used $h \equiv -A \cdot Y$. To complete the correspondence and having as our guideline the one-loop results for the RGEs, μ of [72] should be replaced by our μ and the coupling B of the two

Higgs scalars should be replaced by our $-m_3^2$. With this correspondence the two-loop RGEs are retrieved unambiguously from [72] and are adapted to our notation.

Concerning the neutralino and chargino mass matrices, In the \tilde{B} , $\tilde{W}^{(3)}$, $i\tilde{H}_1^0$, $i\tilde{H}_2^0$, basis the neutralino mass matrix is

$$\mathcal{M}_N = \begin{pmatrix} M_1 & 0 & g' \langle H_1^* \rangle & -g' \langle H_2^* \rangle \\ 0 & M_2 & -g \langle H_1^* \rangle & g \langle H_2^* \rangle \\ g' \langle H_1^* \rangle & -g \langle H_1^* \rangle & 0 & -\mu \\ -g' \langle H_2^* \rangle & g \langle H_2^* \rangle & -\mu & 0 \end{pmatrix}. \quad (\text{A.5})$$

The field dependent neutralino mass matrix entering into the effective potential has a similar form with the Higgs VEVs replaced by the neutral components of the corresponding Higgs doublets. Note that the gaugino masses $M_{1,2}$ the parameter μ as well as the Higgs VEVs are complex in general. Regarding the Higgses one can verify that the mass eigenstates depend only on their relative phase. One can diagonalize the symmetric neutralino mass matrix as

$$\mathcal{O}^T \mathcal{M}_N \mathcal{O} = \text{diag} \left(m_{\tilde{\chi}_1^0}, m_{\tilde{\chi}_2^0}, m_{\tilde{\chi}_3^0}, m_{\tilde{\chi}_4^0} \right), \quad (\text{A.6})$$

where \mathcal{O} is complex in general. In our approach this matrix is chosen in such a way that the eigenvalues $m_{\tilde{\chi}_i^0}$ are real and positive.

The chargino mass matrix can be obtained from the Lagrangian terms

$$\mathcal{L}_{\text{charginos}}^{\text{mass}} = - \left(\tilde{W}^-, i\tilde{H}_1^- \right) \mathcal{M}_c \begin{pmatrix} \tilde{W}^+ \\ i\tilde{H}_2^+ \end{pmatrix} + (h.c.), \quad (\text{A.7})$$

where we have defined $\tilde{W}^\pm \equiv \frac{\tilde{W}^{(1)} \mp i\tilde{W}^{(2)}}{\sqrt{2}}$. The mass matrix is

$$\mathcal{M}_C = \begin{pmatrix} M_2 & -g \langle H_2^* \rangle \\ -g \langle H_1^* \rangle & \mu \end{pmatrix}, \quad (\text{A.8})$$

which can be diagonalized as

$$U \mathcal{M}_C V^\dagger = \begin{pmatrix} m_{\tilde{\chi}_1} & 0 \\ 0 & m_{\tilde{\chi}_2} \end{pmatrix}. \quad (\text{A.9})$$

Thus,

$$\mathcal{L}_{\text{charginos}}^{\text{mass}} = -m_{\tilde{\chi}_1} \tilde{\tilde{\chi}}_1 \tilde{\chi}_1 - m_{\tilde{\chi}_2} \tilde{\tilde{\chi}}_2 \tilde{\chi}_2. \quad (\text{A.10})$$

The Dirac chargino states $\tilde{\chi}_{1,2}$ in this equation are defined by

$$\tilde{\chi}_1 \equiv \begin{pmatrix} \lambda_1^+ \\ \bar{\lambda}_1^- \end{pmatrix}, \quad \tilde{\chi}_2 \equiv \begin{pmatrix} \lambda_2^+ \\ \bar{\lambda}_2^- \end{pmatrix}, \quad (\text{A.11})$$

with the two component Weyl spinors $\lambda_{1,2}^\pm$ related to \tilde{W}^\pm , $i\tilde{H}_1^-$, $i\tilde{H}_2^+$ by

$$V \begin{pmatrix} \tilde{W}^+ \\ i\tilde{H}_2^+ \end{pmatrix} \equiv \begin{pmatrix} \lambda_1^+ \\ \lambda_2^+ \end{pmatrix}, \quad \left(\tilde{W}^-, i\tilde{H}_1^- \right) U^\dagger \equiv (\lambda_1^-, \lambda_2^-). \quad (\text{A.12})$$

The gauge interactions of charginos and neutralinos can be read from the Lagrangian⁸

$$\mathcal{L} = g (W_\mu^+ J_-^\mu + W_\mu^- J_+^\mu) + e A_\mu J_{em}^\mu + \frac{e}{s c} Z_\mu J_Z^\mu. \quad (\text{A.13})$$

In the equation above $s = \sin \theta_W$, $c = \cos \theta_W$. Also,

$$\begin{pmatrix} Z_\mu \\ A_\mu \end{pmatrix} = \begin{pmatrix} c & s \\ -s & c \end{pmatrix} \begin{pmatrix} W_\mu^{(3)} \\ B_\mu \end{pmatrix}. \quad (\text{A.14})$$

The currents J_+^μ , J_{em}^μ and J_Z^μ are given by

$$J_+^\mu \equiv \bar{\tilde{\chi}}_a^0 \gamma^\mu [\mathcal{P}_L \mathcal{P}_{ai}^L + \mathcal{P}_R \mathcal{P}_{ai}^R] \tilde{\chi}_i \quad a = 1..4, \quad i = 1, 2, \quad (\text{A.15})$$

where $\mathcal{P}_{L,R} = \frac{1 \mp \gamma_5}{2}$ and

$$\mathcal{P}_{ai}^L \equiv +\frac{1}{\sqrt{2}} \mathcal{O}_{4a}^* V_{i2}^* - \mathcal{O}_{2a}^* V_{i1}^* \quad , \quad \mathcal{P}_{ai}^R \equiv -\frac{1}{\sqrt{2}} \mathcal{O}_{3a} U_{i2}^* - \mathcal{O}_{2a} U_{i1}^*. \quad (\text{A.16})$$

The electromagnetic current J_{em}^μ is

$$J_{em}^\mu = \tilde{\chi}_1 \gamma^\mu \tilde{\chi}_1 + \tilde{\chi}_2 \gamma^\mu \tilde{\chi}_2. \quad (\text{A.17})$$

Finally, the neutral current J_Z^μ can be read from

$$J_Z^\mu \equiv \bar{\tilde{\chi}}_i^c \gamma^\mu [\mathcal{P}_L \mathcal{A}_{ij}^L + \mathcal{P}_R \mathcal{A}_{ij}^R] \tilde{\chi}_j + \frac{1}{2} \bar{\tilde{\chi}}_a^0 \gamma^\mu [\mathcal{P}_L \mathcal{B}_{ab}^L + \mathcal{P}_R \mathcal{B}_{ab}^R] \tilde{\chi}_b^0, \quad (\text{A.18})$$

with

$$\begin{aligned} \mathcal{A}_{ij}^L &= c^2 \delta_{ij} - \frac{1}{2} V_{i2} V_{j2}^*, \\ \mathcal{A}_{ij}^R &= c^2 \delta_{ij} - \frac{1}{2} U_{i2} U_{j2}^*, \\ \mathcal{B}_{ab}^L &= \frac{1}{2} (\mathcal{O}_{3a}^* \mathcal{O}_{3b} - \mathcal{O}_{4a}^* \mathcal{O}_{4b}), \\ \mathcal{B}_{ab}^R &= -\mathcal{B}_{ab}^{L,*}. \end{aligned} \quad (\text{A.19})$$

The chargino and neutralino couplings to sfermions are given by the following Lagrangian terms

$$\mathcal{L} = i \bar{\tilde{\chi}}_i^c (\mathcal{P}_L a_{ij}^{f' \tilde{f}} + \mathcal{P}_R b_{ij}^{f' \tilde{f}}) f' \tilde{f}_j^* + i \bar{\tilde{\chi}}_i (\mathcal{P}_L a_{ij}^{f \tilde{f}'} + \mathcal{P}_R b_{ij}^{f \tilde{f}'}) f \tilde{f}_j'^* + (h.c.). \quad (\text{A.20})$$

In this, χ_i ($i = 1, 2$) are the positively charged charginos and χ_i^c the corresponding charge conjugate states having opposite charge. f, f' denote “up” and “down” fermions, quarks or leptons, while $\tilde{f}_i, \tilde{f}_i'$ are the corresponding sfermion mass eigenstates. The left and right-handed couplings appearing above are given by

$$\begin{aligned} a_{ij}^{f' \tilde{f}} &= g V_{i1}^* K_{j1}^{\tilde{f}} - h_f V_{i2}^* K_{j2}^{\tilde{f}}, & b_{ij}^{f' \tilde{f}} &= -h_{f'} U_{i2}^* K_{j1}^{\tilde{f}}, \\ a_{ij}^{f \tilde{f}'} &= g U_{i1} K_{j1}^{\tilde{f}'} + h_{f'} U_{i2} K_{j2}^{\tilde{f}'}, & b_{ij}^{f \tilde{f}'} &= h_f V_{i2} K_{j1}^{\tilde{f}'}. \end{aligned}$$

⁸ In our notation $e \equiv$ electron's charge.

In the equation above h_f , $h_{f'}$ are the Yukawa couplings of the up and down fermions respectively. The matrices $K^{\tilde{f}, \tilde{f}'}$ which diagonalize the sfermion mass matrices become the unit matrices in the absence of left-right sfermion mixings. For the electron and muon family the lepton masses are taken to be vanishing in the case that mixings do not occur. In addition the right-handed couplings, are zero.

The corresponding neutralino couplings are given by

$$\mathcal{L} = i \bar{\chi}_a^0 (\mathcal{P}_L a_{aj}^{f\tilde{f}} + \mathcal{P}_R b_{aj}^{f\tilde{f}}) f \tilde{f}_j^* + i \bar{\chi}_a^0 (\mathcal{P}_L a_{aj}^{f'\tilde{f}'} + \mathcal{P}_R b_{aj}^{f'\tilde{f}'}) f' \tilde{f}_j'^* + (h.c). \quad (\text{A.21})$$

The left and right-handed couplings for the up fermions, sfermions are given by

$$\begin{aligned} a_{aj}^{f\tilde{f}} &= \sqrt{2} (g T_f^3 O_{2a} + g' \frac{Y_f}{2} O_{1a}) K_{j1}^f + h_f O_{4a} K_{j2}^f, \\ b_{aj}^{f\tilde{f}} &= \sqrt{2} (-g' \frac{Y_{f^c}}{2} O_{1a}^*) K_{j2}^f - h_f O_{4a}^* K_{j1}^f, \end{aligned}$$

while those for the down fermions and sfermions are given by

$$\begin{aligned} a_{aj}^{f'\tilde{f}'} &= \sqrt{2} (g T_{f'}^3 O_{2a} + g' \frac{Y_{f'}}{2} O_{1a}) K_{j1}^{f'} - h_{f'} O_{3a} K_{j2}^{f'}, \\ b_{aj}^{f'\tilde{f}'} &= \sqrt{2} (-g' \frac{Y_{f'^c}}{2} O_{1a}^*) K_{j2}^{f'} + h_{f'} O_{3a}^* K_{j1}^{f'}. \end{aligned}$$

References

- [1] D. J. H. Chung, L. L. Everett, G. L. Kane, S. F. King, J. D. Lykken and L. T. Wang, Phys. Rept. **407**, 1 (2005) [arXiv:hep-ph/0312378].
- [2] H. E. Haber, Nucl. Phys. Proc. Suppl. **62**, 469 (1998) [arXiv:hep-ph/9709450].
- [3] J. R. Ellis, S. Ferrara and D. V. Nanopoulos, Phys. Lett. B **114**, 231 (1982); W. Buchmuller and D. Wyler, Phys. Lett. B **121**, 321 (1983); J. Polchinski and M. B. Wise, Phys. Lett. B **125**, 393 (1983); M. Dugan, B. Grinstein and L. J. Hall, Nucl. Phys. B **255**, 413 (1985).
- [4] F. del Aguila, M. B. Gavela, J. A. Grifols and A. Mendez, Phys. Lett. B **126**, 71 (1983) [Erratum-ibid. B **129**, 473 (1983)]; E. Franco and M. L. Mangano, Phys. Lett. B **135**, 445 (1984); J. M. Gerard, W. Grimus, A. Raychaudhuri and G. Zoupanos, Phys. Lett. B **140**, 349 (1984); J. M. Gerard, W. Grimus, A. Masiero, D. V. Nanopoulos and A. Raychaudhuri, Nucl. Phys. B **253**, 93 (1985); A. I. Sanda, Phys. Rev. D **32**, 2992 (1985).
- [5] R. Arnowitt, J. L. Lopez and D. V. Nanopoulos, Phys. Rev. D **42**, 2423 (1990); R. Arnowitt, M. J. Duff and K. S. Stelle, Phys. Rev. D **43**, 3085 (1991).
- [6] R. Garisto and J. D. Wells, Phys. Rev. D **55**, 1611 (1997) [arXiv:hep-ph/9609511].
- [7] S. Dimopoulos and S. D. Thomas, Nucl. Phys. B **465**, 23 (1996) [arXiv:hep-ph/9510220];
- [8] D. A. Demir, A. Masiero and O. Vives, Phys. Rev. D **61**, 075009 (2000) [arXiv:hep-ph/9909325]; D. A. Demir, A. Masiero and O. Vives, Phys. Lett. B **479**, 230 (2000) [arXiv:hep-ph/9911337].
- [9] M. Brhlik and G. L. Kane, Phys. Lett. B **437**, 331 (1998) [arXiv:hep-ph/9803391]; P. Langacker, G. Paz, L. T. Wang and I. Yavin, decay,” JHEP **0707** (2007) 055 [arXiv:hep-ph/0702068].
- [10] S. Mrenna, G. L. Kane and L. T. Wang, Phys. Lett. B **483**, 175 (2000) [arXiv:hep-ph/9910477]; S. Y. Choi, A. Djouadi, M. Guchait, J. Kalinowski, H. S. Song and P. M. Zerwas, Eur. Phys. J. C **14**, 535 (2000) [arXiv:hep-ph/0002033]; V. D. Barger, T. Han, T. J. Li and T. Plehn, Phys. Lett. B **475**, 342 (2000) [arXiv:hep-ph/9907425]; V. D. Barger, T. Han and J. Jiang, Phys. Rev. D **63**, 075002 (2001) [arXiv:hep-ph/0006223]; S. Y. Choi, J. Kalinowski, G. Moortgat-Pick and P. M. Zerwas, arXiv:hep-ph/0202039; J. Kalinowski and G. Moortgat-Pick, in *Proc. of the APS/DPF/DPB Summer Study on the Future of Particle Physics (Snowmass 2001)* ed. N. Graf, eConf **C010630**, P323 (2001) [arXiv:hep-ph/0202083].
- [11] P. G. Harris *et al.*, Phys. Rev. Lett. **82**, 904 (1999).
- [12] B. C. Regan, E. D. Commins, C. J. Schmidt and D. DeMille, Phys. Rev. Lett. **88**, 071805 (2002).

- [13] M. V. Romalis, W. C. Griffith and E. N. Fortson, Phys. Rev. Lett. **86**, 2505 (2001) [arXiv:hep-ex/0012001].
- [14] T. Falk and K. A. Olive, Phys. Lett. B **375**, 196 (1996) [arXiv:hep-ph/9602299]; Phys. Lett. B **439**, 71 (1998) [arXiv:hep-ph/9806236].
- [15] T. Ibrahim and P. Nath, Phys. Lett. B **418**, 98 (1998) [arXiv:hep-ph/9707409]; T. Ibrahim and P. Nath, Phys. Rev. D **57**, 478 (1998) [Erratum-ibid. D **58**, 019901 (1998 ERRAT,D60,079903.1999 ERRAT,D60,119901.1999)] [arXiv:hep-ph/9708456].
- [16] T. Ibrahim and P. Nath, Phys. Rev. D **58**, 111301 (1998) [Erratum-ibid. D **60**, 099902 (1999)] [arXiv:hep-ph/9807501].
- [17] T. Falk, A. Ferstl and K. A. Olive, Phys. Rev. D **59**, 055009 (1999) [Erratum-ibid. D **60**, 119904 (1999)] [arXiv:hep-ph/9806413]; T. Falk, arXiv:hep-ph/0001207; T. Falk, A. Ferstl and K. A. Olive, Astropart. Phys. **13**, 301 (2000) [arXiv:hep-ph/9908311].
- [18] M. Brhlik, G. J. Good and G. L. Kane, Phys. Rev. D **59**, 115004 (1999) [arXiv:hep-ph/9810457]; A. Bartl, T. Gajdosik, W. Porod, P. Stockinger and H. Stremnitzer, Phys. Rev. D **60**, 073003 (1999) [arXiv:hep-ph/9903402]; S. Pokorski, J. Rosiek and C. A. Savoy, Nucl. Phys. B **570**, 81 (2000) [arXiv:hep-ph/9906206]; R. Arnowitt, B. Dutta and Y. Santoso, Phys. Rev. D **64**, 113010 (2001) [arXiv:hep-ph/0106089].
- [19] T. Falk, K. A. Olive, M. Pospelov and R. Roiban, Nucl. Phys. B **560**, 3 (1999) [arXiv:hep-ph/9904393]; V. D. Barger, T. Falk, T. Han, J. Jiang, T. Li and T. Plehn, Phys. Rev. D **64**, 056007 (2001) [arXiv:hep-ph/0101106]; S. Abel, S. Khalil and O. Lebedev, Nucl. Phys. B **606**, 151 (2001) [arXiv:hep-ph/0103320].
- [20] T. Ibrahim and P. Nath, Phys. Rev. D **61**, 093004 (2000) [arXiv:hep-ph/9910553].
- [21] M. Brhlik, L. L. Everett, G. L. Kane and J. D. Lykken, Phys. Rev. Lett. **83**, 2124 (1999) [arXiv:hep-ph/9905215]; M. Brhlik, L. L. Everett, G. L. Kane and J. D. Lykken, Phys. Rev. D **62**, 035005 (2000) [arXiv:hep-ph/9908326]; S. Abel, S. Khalil and O. Lebedev, Phys. Rev. Lett. **86**, 5850 (2001) [arXiv:hep-ph/0103031].
- [22] P. Nath, Phys. Rev. Lett. **66** (1991) 2565. Y. Kizukuri and N. Oshimo, Phys. Rev. D **45**, 1806 (1992); Y. Kizukuri and N. Oshimo, Phys. Rev. D **46**, 3025 (1992); A. G. Cohen, D. B. Kaplan and A. E. Nelson, Phys. Lett. B **388**, 588 (1996) [arXiv:hep-ph/9607394].
- [23] A. Pilaftsis, Phys. Lett. B **471**, 174 (1999) [arXiv:hep-ph/9909485];
- [24] O. Lebedev and M. Pospelov, Phys. Rev. Lett. **89**, 101801 (2002) [arXiv:hep-ph/0204359].
- [25] D. Chang, W. Y. Keung and A. Pilaftsis, Phys. Rev. Lett. **82**, 900 (1999) [Erratum-ibid. **83**, 3972 (1999)] [arXiv:hep-ph/9811202]; D. Chang, W. F. Chang and W. Y. Keung, Phys. Rev. D **66**, 116008 (2002) [arXiv:hep-ph/0205084]; A. Pilaftsis, Nucl. Phys. B **644**, 263 (2002) [arXiv:hep-ph/0207277].

- [26] W. J. Marciano and A. Queijeiro, Phys. Rev. D **33**, 3449 (1986); T. Kadoyoshi and N. Oshimo, Phys. Rev. D **55**, 1481 (1997) [arXiv:hep-ph/9607301]; N. G. Deshpande and J. Jiang, Phys. Lett. B **615**, 111 (2005) [arXiv:hep-ph/0503116].
- [27] A. Pilaftsis, Phys. Rev. D **62**, 016007 (2000) [arXiv:hep-ph/9912253].
- [28] D. Chang, W. F. Chang and W. Y. Keung, Phys. Rev. D **71**, 076006 (2005) [arXiv:hep-ph/0503055].
- [29] G. F. Giudice and A. Romanino, Phys. Lett. B **634**, 307 (2006) [arXiv:hep-ph/0510197].
- [30] K. A. Olive, M. Pospelov, A. Ritz and Y. Santoso, Phys. Rev. D **72**, 075001 (2005) [arXiv:hep-ph/0506106].
- [31] U. Chattopadhyay, T. Ibrahim and D. P. Roy, Phys. Rev. D **64**, 013004 (2001) [arXiv:hep-ph/0012337]; D. A. Demir, O. Lebedev, K. A. Olive, M. Pospelov and A. Ritz, Nucl. Phys. B **680**, 339 (2004) [arXiv:hep-ph/0311314]; S. Oshima, T. Nihei and T. Fujita, J. Phys. Soc. Jap. **74**, 2480 (2005) [arXiv:hep-ph/0501236].
- [32] M. Pospelov and A. Ritz, Annals Phys. **318**, 119 (2005) [arXiv:hep-ph/0504231].
- [33] J. Erler and M. J. Ramsey-Musolf, Prog. Part. Nucl. Phys. **54**, 351 (2005) [arXiv:hep-ph/0404291].
- [34] S. M. Barr and A. Zee, Phys. Rev. Lett. **65**, 21 (1990) [Erratum-ibid. **65**, 2920 (1990)].
- [35] A. Pilaftsis, Phys. Rev. D **58**, 096010 (1998) [arXiv:hep-ph/9803297]; Phys. Lett. B **435**, 88 (1998) [arXiv:hep-ph/9805373]; A. Pilaftsis and C. E. M. Wagner, Nucl. Phys. B **553**, 3 (1999) [arXiv:hep-ph/9902371]; M. Carena, J. R. Ellis, S. Mrenna, A. Pilaftsis and C. E. M. Wagner, Nucl. Phys. B **659**, 145 (2003) [arXiv:hep-ph/0211467]; J. S. Lee, A. Pilaftsis, M. Carena, S. Y. Choi, M. Drees, J. R. Ellis and C. E. M. Wagner, Comput. Phys. Commun. **156**, 283 (2004) [arXiv:hep-ph/0307377].
- [36] M. Carena, J. R. Ellis, A. Pilaftsis and C. E. M. Wagner, Nucl. Phys. B **586**, 92 (2000) [arXiv:hep-ph/0003180]; M. Carena, J. R. Ellis, A. Pilaftsis and C. E. M. Wagner, Phys. Lett. B **495**, 155 (2000) [arXiv:hep-ph/0009212]; M. S. Carena, J. R. Ellis, A. Pilaftsis and C. E. M. Wagner, Nucl. Phys. B **625**, 345 (2002) [arXiv:hep-ph/0111245].
- [37] K. S. Babu, C. F. Kolda, J. March-Russell and F. Wilczek, Phys. Rev. D **59**, 016004 (1999) [arXiv:hep-ph/9804355]; S. Y. Choi, M. Drees and J. S. Lee, Phys. Lett. B **481**, 57 (2000) [arXiv:hep-ph/0002287]; S. Heinemeyer, Eur. Phys. J. C **22**, 521 (2001) [arXiv:hep-ph/0108059].
- [38] T. Ibrahim and P. Nath, Phys. Rev. D **63**, 035009 (2001) [arXiv:hep-ph/0008237]; T. Ibrahim, Phys. Rev. D **64**, 035009 (2001) [arXiv:hep-ph/0102218]; T. Ibrahim and P. Nath, Phys. Rev. D **66**, 015005 (2002) [arXiv:hep-ph/0204092].

- [39] A. Dedes and S. Moretti, Nucl. Phys. B **576**, 29 (2000) [arXiv:hep-ph/9909418]; Phys. Rev. Lett. **84**, 22 (2000) [arXiv:hep-ph/9908516]; S. Y. Choi and J. S. Lee, Phys. Rev. D **61**, 115002 (2000) [arXiv:hep-ph/9910557]; B. Grzadkowski, J. F. Gunion and J. Kalinowski, Phys. Lett. B **480**, 287 (2000) [arXiv:hep-ph/0001093]; G. L. Kane and L. T. Wang, Phys. Lett. B **488**, 383 (2000) [arXiv:hep-ph/0003198]; E. Christova, H. Eberl, W. Majerotto and S. Kraml, Nucl. Phys. B **639**, 263 (2002) [Erratum-ibid. B **647**, 359 (2002)] [arXiv:hep-ph/0205227]; M. Carena and H. E. Haber, Prog. Part. Nucl. Phys. **50**, 63 (2003) [arXiv:hep-ph/0208209]; E. Christova, H. Eberl, W. Majerotto and S. Kraml, JHEP **0212**, 021 (2002) [arXiv:hep-ph/0211063].
- [40] B. Grzadkowski and J. F. Gunion, Phys. Lett. B **350**, 218 (1995) [arXiv:hep-ph/9501339]; D. Atwood and A. Soni, Phys. Rev. D **52**, 6271 (1995) [arXiv:hep-ph/9505233]; A. Pilaftsis, Phys. Rev. Lett. **77**, 4996 (1996) [arXiv:hep-ph/9603328]; Nucl. Phys. B **504**, 61 (1997) [arXiv:hep-ph/9702393]; S. Y. Choi and J. S. Lee, Phys. Rev. D **61**, 015003 (2000) [arXiv:hep-ph/9907496]; E. Asakawa, S. Y. Choi and J. S. Lee, Phys. Rev. D **63**, 015012 (2001) [arXiv:hep-ph/0005118]; S. Y. Choi, K. Hagiwara and J. S. Lee, Phys. Rev. D **64**, 032004 (2001) [arXiv:hep-ph/0103294]; M. S. Berger, Phys. Rev. Lett. **87**, 131801 (2001) [arXiv:hep-ph/0105128]; A. G. Akeroyd and A. Arhrib, Phys. Rev. D **64**, 095018 (2001) [arXiv:hep-ph/0107040].
- [41] S. Y. Choi, K. Hagiwara and J. S. Lee, Phys. Lett. B **529**, 212 (2002) [arXiv:hep-ph/0110138]; A. Arhrib, D. K. Ghosh and O. C. W. Kong, Phys. Lett. B **537**, 217 (2002) [arXiv:hep-ph/0112039]; C. Blochinger *et al.*, arXiv:hep-ph/0202199; S. Y. Choi, M. Drees, J. S. Lee and J. Song, Eur. Phys. J. C **25**, 307 (2002) [arXiv:hep-ph/0204200]; S. W. Ham, S. K. Oh, E. J. Yoo, C. M. Kim and D. Son, Phys. Rev. D **68**, 055003 (2003) [arXiv:hep-ph/0205244]; S. Y. Choi, B. c. Chung, P. Ko and J. S. Lee, Phys. Rev. D **66**, 016009 (2002) [arXiv:hep-ph/0206025].
- [42] S. Kraml *et al.*, arXiv:hep-ph/0608079.
- [43] M. Fukugita and T. Yanagida, Phys. Lett. B **174**, 45 (1986).
- [44] A.G. Cohen, D.B. Kaplan and A.E. Nelson, *Ann. Rev. Nucl. Part. Sci.* **43** (1993) 27; M. Quirós, *Helv. Phys. Acta* **67** (1994) 451; V.A. Rubakov and M.E. Shaposhnikov, *Phys. Usp.* **39** (1996) 461; M. Carena and C.E.M. Wagner, hep-ph/9704347; A. Riotto, M. Trodden, *Ann. Rev. Nucl. Part. Sci.* **49** (1999) 35; M. Quirós and M. Seco, *Nucl. Phys. B Proc. Suppl.* **81** (2000) 63, hep-ph/9703274.
- [45] M. S. Carena, M. Quiros and C. E. M. Wagner, Phys. Lett. B **380**, 81 (1996) [arXiv:hep-ph/9603420]; D. Delepine, J. M. Gerard, R. Gonzalez Felipe and J. Weyers, Phys. Lett. B **386**, 183 (1996) [arXiv:hep-ph/9604440]; J. M. Cline and G. D. Moore, Phys. Rev. Lett. **81**, 3315 (1998) [arXiv:hep-ph/9806354].
- [46] M. S. Carena, M. Quiros and C. E. M. Wagner, Nucl. Phys. B **524**, 3 (1998) [arXiv:hep-ph/9710401].

- [47] M. S. Carena, M. Quiros, A. Riotto, I. Vilja and C. E. M. Wagner, Nucl. Phys. B **503**, 387 (1997) [arXiv:hep-ph/9702409]; M. S. Carena, J. M. Moreno, M. Quiros, M. Seco and C. E. M. Wagner, Nucl. Phys. B **599**, 158 (2001) [arXiv:hep-ph/0011055].
- [48] M. Laine and K. Rummukainen, Nucl. Phys. B **535**, 423 (1998) [arXiv:hep-lat/9804019]; M. Laine and K. Rummukainen, Nucl. Phys. B **597**, 23 (2001) [arXiv:hep-lat/0009025]; M. Laine, arXiv:hep-ph/0010275.
- [49] C. Balazs, M. S. Carena and C. E. M. Wagner, Phys. Rev. D **70**, 015007 (2004) [arXiv:hep-ph/0403224]; C. Balazs, M. S. Carena, A. Menon, D. E. Morrissey and C. E. M. Wagner, Phys. Rev. D **71**, 075002 (2005) [arXiv:hep-ph/0412264].
- [50] V. Cirigliano, S. Profumo and M. J. Ramsey-Musolf, JHEP **0607**, 002 (2006) [arXiv:hep-ph/0603246].
- [51] C. Lee, V. Cirigliano and M. J. Ramsey-Musolf, Phys. Rev. D **71**, 075010 (2005) [arXiv:hep-ph/0412354].
- [52] C. L. Bennett *et al.* [WMAP Collaboration], Astrophys. J. Suppl. **148**, 1 (2003) [arXiv:astro-ph/0302207].
- [53] D. N. Spergel *et al.* [WMAP Collaboration], Astrophys. J. Suppl. **148**, 175 (2003) [arXiv:astro-ph/0302209].
- [54] D. N. Spergel *et al.* [WMAP Collaboration], Astrophys. J. Suppl. **170**, 377 (2007) [arXiv:astro-ph/0603449].
- [55] M. Tegmark *et al.* [SDSS Collaboration], Phys. Rev. D **69**, 103501 (2004) [arXiv:astro-ph/0310723].
- [56] A. B. Lahanas, N. E. Mavromatos and D. V. Nanopoulos, Int. J. Mod. Phys. D **12**, 1529 (2003) [arXiv:hep-ph/0308251].
- [57] T. Falk, K. A. Olive and M. Srednicki, Phys. Lett. B **354**, 99 (1995) [arXiv:hep-ph/9502401].
- [58] G. Belanger, F. Boudjema, S. Kraml, A. Pukhov and A. Semenov, Phys. Rev. D **73**, 115007 (2006) [arXiv:hep-ph/0604150].
- [59] G. Belanger, F. Boudjema, S. Kraml, A. Pukhov and A. Semenov, AIP Conf. Proc. **878**, 46 (2006) [arXiv:hep-ph/0610110].
- [60] D. A. Demir, Phys. Rev. D **60**, 055006 (1999) [arXiv:hep-ph/9901389].
- [61] D. A. Demir, Phys. Rev. D **60**, 095007 (1999) [arXiv:hep-ph/9905571].
- [62] M. E. Gomez, T. Ibrahim, P. Nath and S. Skadhauge, arXiv:hep-ph/0410007.
- [63] M. E. Gomez, T. Ibrahim, P. Nath and S. Skadhauge, Phys. Rev. D **70**, 035014 (2004) [arXiv:hep-ph/0404025].

- [64] M. E. Gomez, T. Ibrahim, P. Nath and S. Skadhauge, *Prepared for IDM 2004: 5th International Workshop on the Identification of Dark Matter, Edinburgh, Scotland, United Kingdom, 6-10 Sep 2004*.
- [65] M. Argyrou, A. B. Lahanas, D. V. Nanopoulos and V. C. Spanos, Phys. Rev. D **70**, 095008 (2004) [Erratum-ibid. D **70**, 119902 (2004)] [arXiv:hep-ph/0404286].
- [66] M. E. Gomez, T. Ibrahim, P. Nath and S. Skadhauge, Phys. Rev. D **72**, 095008 (2005) [arXiv:hep-ph/0506243].
- [67] P. Nath, J. z. Wu and R. Arnowitt, Phys. Rev. D **52**, 4169 (1995) [arXiv:hep-ph/9502388].
- [68] E. Brubaker *et al.* [Tevatron Electroweak Working Group], arXiv:hep-ex/0608032;
- [69] [CDF Collaboration], arXiv:hep-ex/0703034.
- [70] M. Drees and M. M. Nojiri, Phys. Rev. D **47** (1993) 376 [arXiv:hep-ph/9207234]; H. Baer and M. Brhlik, Phys. Rev. D **53** (1996) 597 [arXiv:hep-ph/9508321]; A. B. Lahanas, D. V. Nanopoulos and V. C. Spanos, Phys. Rev. D **62** (2000) 023515 [arXiv:hep-ph/9909497]; Mod. Phys. Lett. A **16** (2001) 1229 [arXiv:hep-ph/0009065]; H. Baer, M. Brhlik, M. A. Diaz, J. Ferrandis, P. Mercadante, P. Quintana and X. Tata, Phys. Rev. D **63** (2001) 015007 [arXiv:hep-ph/0005027]; J. R. Ellis, T. Falk, G. Ganis, K. A. Olive and M. Srednicki, Phys. Lett. B **510** (2001) 236 [arXiv:hep-ph/0102098].
- [71] A. B. Lahanas and V. C. Spanos, Eur. Phys. J. C **23** (2002) 185 [arXiv:hep-ph/0106345]; J. R. Ellis, K. A. Olive, Y. Santoso and V. C. Spanos, Phys. Rev. D **69** (2004) 095004 [arXiv:hep-ph/0310356].
- [72] S. P. Martin and M. T. Vaughn, Phys. Rev. D **50**, 2282 (1994) [arXiv:hep-ph/9311340].
- [73] Y. Yamada, Phys. Rev. D **50**, 3537 (1994) [arXiv:hep-ph/9401241].
- [74] L. J. Hall, R. Rattazzi and U. Sarid, Phys. Rev. D **50**, 7048 (1994) [arXiv:hep-ph/9306309]; Phys. Rev. D **53**, 1553 (1996) [arXiv:hep-ph/9505428]; R. Hempfling, Phys. Rev. D **49**, 6168 (1994); M. S. Carena, M. Olechowski, S. Pokorski and C. E. M. Wagner, Nucl. Phys. B **426**, 269 (1994) [arXiv:hep-ph/9402253].
- [75] M. S. Carena, D. Garcia, U. Nierste and C. E. M. Wagner, Nucl. Phys. B **577**, 88 (2000) [arXiv:hep-ph/9912516].
- [76] T. Ibrahim and P. Nath, Phys. Rev. D **67**, 095003 (2003) [Erratum-ibid. D **68**, 019901 (2003)] [arXiv:hep-ph/0301110].
- [77] K. G. Chetyrkin, Phys. Lett. B **404**, 161 (1997) [arXiv:hep-ph/9703278].
- [78] G. Martinelli and C. T. Sachrajda, Nucl. Phys. B **559**, 429 (1999) [arXiv:hep-lat/9812001].

- [79] D. M. Pierce, J. A. Bagger, K. T. Matchev and R. j. Zhang, Nucl. Phys. B **491**, 3 (1997) [arXiv:hep-ph/9606211].
- [80] S. P. Martin and M. T. Vaughn, Phys. Lett. B **318** (1993) 331 [arXiv:hep-ph/9308222].
- [81] Y. Yamada, Phys. Lett. B **623** (2005) 104 [arXiv:hep-ph/0506262].
- [82] S. P. Martin, Phys. Rev. D **72**, 096008 (2005) [arXiv:hep-ph/0509115].
- [83] J. R. Ellis, T. Falk and K. A. Olive, Phys. Lett. B **444** (1998) 367; J. R. Ellis, T. Falk, K. A. Olive and M. Srednicki, Astropart. Phys. **13** (2000) 181 [Erratum-ibid. **15**, 413 (2001)] [arXiv:hep-ph/9905481]; M. E. Gomez, G. Lazarides and C. Pallis, Phys. Rev. D **61** (2000) 123512; R. Arnowitt, B. Dutta and Y. Santoso, Nucl. Phys. B **606** (2001) 59 [arXiv:hep-ph/0102181]; T. Nihei, L. Roszkowski and R. Ruiz de Austri, JHEP **0207** (2002) 024 [arXiv:hep-ph/0206266]; J. Edsjo, M. Schelke, P. Ullio and P. Gondolo, JCAP **0304**, 001 (2003) [arXiv:hep-ph/0301106].
- [84] K. L. Chan, U. Chattopadhyay and P. Nath, Phys. Rev. D **58** (1998) 096004 [arXiv:hep-ph/9710473]; J. L. Feng, K. T. Matchev and T. Moroi, Phys. Rev. Lett. **84** (2000) 2322 [arXiv:hep-ph/9908309]; J. L. Feng, K. T. Matchev and T. Moroi, Phys. Rev. D **61** (2000) 075005 [arXiv:hep-ph/9909334]; J. L. Feng, K. T. Matchev and F. Wilczek, Phys. Lett. B **482** (2000) 388 [arXiv:hep-ph/0004043].
- [85] M. Frank, T. Hahn, S. Heinemeyer, W. Hollik, H. Rzehak and G. Weiglein, JHEP **0702** (2007) 047 [arXiv:hep-ph/0611326]; S. Heinemeyer, W. Hollik and G. Weiglein, Eur. Phys. J. C **9** (1999) 343 [arXiv:hep-ph/9812472].
- [86] J. R. Ellis and F. Zwirner, Nucl. Phys. B **338**, 317 (1990).